The Greenhouse Effect and the Infrared Radiative Structure of the Earth's Atmosphere

Ferenc Mark Miskolczi

Geodetic and Geophysical Institute, Hungarian Academy of Sciences, Csatkai Endre u. 6-8, 9400 Sopron, Hungary
fmiskolczi@cox.net

Abstract

This paper presents observed atmospheric thermal and humidity structures and global scale simulations of the infrared absorption properties of the Earth's atmosphere. These data show that the global average clear sky greenhouse effect has remained unchanged with time. A theoretically predicted infrared optical thickness is fully consistent with, and supports the observed value. It also facilitates the theoretical determination of the planetary radiative equilibrium cloud cover, cloud altitude and Bond albedo. In steady state, the planetary surface (as seen from space) shows no greenhouse effect: the all-sky surface upward radiation is equal to the available solar radiation. The all-sky climatological greenhouse effect (the difference of the all-sky surface upward flux and absorbed solar flux) at this surface is equal to the reflected solar radiation. The planetary radiative balance is maintained by the equilibrium cloud cover which is equal to the theoretical equilibrium clear sky transfer function. The Wien temperature of the all-sky emission spectrum is locked closely to the thermodynamic triple point of the water assuring the maximum radiation entropy. The stability and natural fluctuations of the global average surface temperature of the heterogeneous system are ultimately determined by the phase changes of water. Many authors have proposed a greenhouse effect due to anthropogenic carbon dioxide emissions. The present analysis shows that such an effect is impossible.

Keywords

Greenhouse Effect; Radiative Transfer; Global Warming

Introduction

In steady state planetary radiative balance the relationship that links the short wave (SW) solar radiation to the long wave (LW) terrestrial or infrared (IR) radiation may be expressed as : $OLR^A = (1-\alpha_B) F_E$. Here OLR^A is the all-sky outgoing LW radiation, $\alpha_B = F_R / F_E$ is the Bond albedo, F_R is the all-sky reflected SW radiation, $F_E = F_0 / 4$ is the available SW radiation over a unit area at the top of the atmosphere (TOA), and F_0 is the solar constant at the Earth's orbit. Isolated planets without any internal heat source must obey the energy conservation principle, therefore the $F_E = F_A + F_R$ and $F_A = OLR^A$ relationships must hold, where F_A is the long term global average absorbed SW radiation in the system. The balance relationship does not suggest anything about how, when, and why the observed thermal energy of the planet is attained during the evolution of the planet. The only meaning of the balance equation is the equality between the thermal energy lost to space and the gained radiative energy by SW absorption when a steady state has been reached.

In a planetary atmosphere with condensing greenhouse gases (GHGs), the active surface that is relevant to the radiative balance equation is the combined clear and cloudy surfaces as seen from space. The ratio of the overcast areas to the total surface area of the planet is called geometric cloud fraction, β . Because of the extreme variability of the planetary cloud cover, the accurate estimation of β from surface or satellite observations is one of the most challenging problems of climate science. The characteristic global average altitude of the cloud top, h^C , is also not known with very high accuracy. Missing from climate science literature are the quantitative theoretical constraints on the value of the β and h^C parameters. These issues will be discussed later in detail.

Cloud layers at any altitude present material discontinuity in the atmospheric vertical structure which disrupts the propagation of the LW radiation. In principle, the global average LW upward radiation from the ground surface, S_U , may be estimated reasonably well from ground surface temperature records. Over cloudy areas, however, the upward IR flux density from the cloud top, S_U^C , cannot be easily measured. The S_U from overcast areas does not contribute to the total OLR^A : $OLR^A = (1-\beta) OLR + \beta OLR^C$, where OLR is the clear sky, and OLR^C is the cloudy sky outgoing LW radiation. Estimations of OLR^C from a unit cloudy area must rely on the observed h^C ,

therefore they are inherently inaccurate. The radiative equilibrium constraint for the clear and cloudy areas are expressed as: $S_U = OLR / f = OLR\,(1+\tau_A+T_A)/2$, and $S_U^C = OLR^C / f^C = OLR^C\,(1+\tau_A^C+T_A^C)/2$, where τ_A, T_A, and f are the flux optical thickness, flux transmittance, and transfer function respectively, and the superscripts indicate the cloudy condition, see Miskolczi (2004, 2007, and 2010). Further on we shall frequently make reference to these publications as M04, M07, and M10. The breakthrough in the quantitative greenhouse science happened in 2007, when the correct mathematical relationship among S_U, OLR, and τ_A for semitransparent atmospheres was first published in M07. The theoretical derivation of the $S_U = OLR / f$ analytical function was the missing link which, through the transfer function and flux optical thickness, connects the surface temperature to the GHG content of the atmosphere.

Here one has to be careful with the computation of S_U from the related ground surface thermodynamic temperature, t_G. For non-black surfaces, the upward radiation is defined by the skin temperature t_S: $S_U = \sigma t_S^4 = \varepsilon_G \sigma t_G^4 < S_G$, where ε_G is the surface flux emissivity, $\sigma = 5.67\times10^{-8}$ Wm^{-2}K^{-4} is the Stefan-Boltzmann constant. $S_G = B(t_G) = B_G$ is the total flux density radiated into the hemisphere from an ideal blackbody radiator at t_G temperature. In planetary radiative budget studies $\varepsilon_G = 1$, and $S_U = S_G$ are usually assumed. For reference, in Trenberth, Fasullo, and Kiehl (2009) (TFK09) the broadband emissivity of the water is $\varepsilon_G = 0.9907$ and the ISCCP-FD t_G is 288.70 K.

The clear and cloudy sky LW downward atmospheric emittance to the ground surface and cloud top are E_D and E_D^C respectively. The all-sky LW downward flux to the ground surface is the sum of the clear and cloudy components: $E_D^A = (1-\beta)\,E_D + \beta\,OLR^{Cd}$, where $OLR^{Cd} = S_T^{Cd} + E_D^{Cd}$ is the cloudy sky contribution. Here S_T^{Cd} is the downward transmitted flux from the cloud bottom, and E_D^{Cd} is the downward atmospheric emission from below the cloud layer. S_D^C is the downward radiation emitted by the cloud bottom, and by definition, $A_A^{Cd} = S_D^C - S_T^{Cd}$ is the absorbed part of S_D^C. Assuming a thin opaque cloud layer the upward and downward radiation (emitted by the cloud deck) are equal, $S_D^C = S_U^C$. The last important flux density component in the cloudy atmosphere is the total upward radiation (transmitted from the surface plus emitted by the atmosphere) at the altitude of the cloud bottom: $OLR^{Cu} = S_T^{Cu} + E_U^{Cu}$. The absorbed surface upward flux at the cloud bottom is $A_A^{Cu} = S_U - S_T^{Cu}$.

Greenhouse Effect

The planetary greenhouse effect (GE) may be defined or quantified in different ways. In astrophysics the all-sky GE is defined via the total available solar radiation interacting with the system: $G^A = S_U^A - F_E$, where $S_U^A = (1-\beta)\,S_U + \beta\,S_U^C$ is the all-sky global average surface upward flux (from the active surface). Similarly to S_U^A, G^A may be obtained from the weighted sum of the clear sky and cloudy sky greenhouse effects: $G^A = (1-\beta)\,G + \beta\,G^C$, where $G = S_U - OLR$, and $G^C = S_U^C - OLR^C$.

In a semi-transparent clear atmosphere, OLR is the sum of the transmitted flux density from the surface, S_T and the atmospheric upward emittance, E_U: $OLR = S_T + E_U$. In a clear, absorbing GHG atmosphere, $S_U = S_T + A_A$ and from the definition of G, follows the $S_U - OLR = A_A - E_U$ greenhouse identity. Here A_A is the clear sky absorbed S_U. Likewise, the greenhouse identity for the fluxes above the cloud top is $S_U^C - OLR^C = A_A^C - E_U^C$, where A_A^C is the absorbed S_U^C above the cloud layer and E_U^C is the upward emission of the air from above the cloud top. For all-sky fluxes, the $S_U^A - OLR^A = A_A^A - E_U^A$ relationship must be satisfied as well. By definition, the all-sky, S_T^A, and the cloudy sky, S_T^C, transmitted fluxes are: $S_T^A = S_U^A - A_A^A$, and $S_T^C = S_U^C - A_A^C$, respectively. $A_A^A = (1-\beta)\,A_A + \beta\,A_A^C$ is the all-sky absorbed LW radiation (above the active surface). In accurate planetary radiative transfer (RT) computations, the greenhouse identities must be observed. The normalized all-sky, clear sky and cloudy sky greenhouse factors (GFs) are the $g^A = G^A / S_U^A$, $g = G / S_U$, and the $g^C = G^C / S_U^C$ ratios respectively. Here g^A is not a simple weighted average: $g^A = g / (1+\beta S_U^C / (1-\beta) / S_U) + g^C / (1+(1-\beta) S_U / \beta / S_U^C)$.

It is anticipated that the thermal structure of the atmosphere is always affected by both the local, and the ever-present global average cloud cover. In terms of the quasi all-sky protocol, clear sky computations of the flux density components are conducted ignoring

the possible (random) presence of the cloud cover. The computed global average fluxes are assumed to implicitly represent the global average cloud condition. In fact, in climate science the classic definition of the greenhouse warming (as the difference of the all-sky global average surface temperature and the planetary emission temperature) is a version of the quasi all-sky protocol.

In the case of planetary radiative equilibrium the global average net energy flux of non-radiative origin (conduction, convection, advection, turbulent mixing, etc.) between the solid and liquid surfaces and the atmosphere must be zero. Of course, the net latent heat release at the boundary layer must be treated as of radiative origin. In global radiative equilibrium $S_U^A = F_E$, $OLR^A = F_A$, $G^A = F_R$, $g^A = \alpha_B$, $\beta = f(\tau_A^T)$, $S_U = OLR / f(\tau_A^T)$, $OLR = A_A^C$, and $OLR^C = E_D^C$, where $\tau_A^T = 1.876$ is the planetary equilibrium flux optical thickness. Note, that the last four relationships are derived theoretically in M07. It is assumed, that the equilibrium atmospheric structure is such, that the cloud cover alone is able to maintain the planetary radiative balance. At the TOA one may write the theoretical equilibrium cloud fraction and the Bond albedo in the simple forms of $\beta = (G - \alpha_B F_E) / (G - G^C)$, and $\alpha_B = (G - \beta(G - G^C)) / F_E$.

In climate science, the all-sky and clear sky greenhouse parameters are defined through the OLR , OLR^A , and S_G fluxes: $G_m^A = S_G - OLR^A$, $G_m = S_G - OLR$, $g_m^A = G_m^A / S_G$, and $g_m = G_m / S_G$. G_m and g_m are the clear sky GE and GF, Ramanathan and Inamdar (2006) (RI06). Sometimes g_m is called as 'normalized trapping' of S_G . We have seen already, that without a realistic ε_G the t_G temperature alone is not sufficient to convert S_G to accurate S_U . Further on, one should notice, that G_m^A , G_m , g_m^A , and g_m are mixed physical quantities and they cannot be associated with either clear, or cloud covered surfaces. To handle the cloud problem, the so-called LW cloud forcing as the difference of the clear and all-sky TOA terrestrial radiation is also introduced: $C_L = OLR - OLR^A$. The frequently used total greenhouse effect terminology in climate science means that $G_m^A = G_m + C_L = S_G - OLR^A$. Although both S_G and OLR^A may easily be observed, G_m^A cannot be related directly to the GHG composition of the atmosphere, and it has no clear physical meaning. The cloud cover has nothing to do with the absorption of the GHGs. Water droplets just like other solid or liquid surfaces radiate continuous IR spectra. The greenhouse effect from the GHGs above the cloud layers should also be taken into account.

The GE based anthropogenic global warming (AGW) hypothesis rests on the assumption that increasing atmospheric CO_2 concentration of human origin will result in increasing global average ground surface temperature. The motivations for writing this paper are the accumulating evidences that GE in the Earth's atmosphere is not a free parameter. AGW estimates based on the classic greenhouse effect explanations of Fourier, Arrhenius, Tyndall, or the Intergovernmental Panel on Climate Change (IPCC) are misleading. The well known, and widely used, semi-infinite opaque formulas with their predicted surface temperature discontinuity cannot be used for semi-transparent atmospheres. AGW predictions, based on modelling calculations for CO_2 doubling, are also not consistent with the observed global average surface temperature records of the last decades. Furthermore, observed local or regional warmings that are usually attributed to greenhouse warming (like Arctic warming) may be accounted for by quite natural causes, see Arrak (2010, 2011).

In this paper, the published atmospheric greenhouse effect and global warming related articles that appeared in the climate science literature, are not reviewed. There are excellent articles summarizing the level of the general understanding (or misunderstanding) of the phenomenon, see Herzberg (2009), Kimoto (2009), Gerlich and Tscheuschner (2009), Van Andel (2010), Hansen et al. (1981), Ramanathan (1981), Raval and Ramanathan (1989) , Lindzen, (2007), Lacis et al. (2010), and Pierrehumbert (2011). The usually quoted quantities are the $G_m^A = \sigma t_G^4 - \sigma t_A^4 = 150$ Wm^{-2} all-sky GE and the $\Delta t_m^A = t_G - t_A = 33$ K greenhouse warming. Here $t_G = 288$ K is the all-sky global average ground surface temperature, $\sigma t_G^4 = 390$ Wm^{-2} is the surface upward radiation, $t_E = (F_E / \sigma)^{1/4} = 279$ K is the planetary effective (or equivalent blackbody) temperature $t_A = (OLR^A / \sigma)^{1/4} = 255$ K is the planetary emission temperature, $F_E = 342$ Wm^{-2}, and $OLR^A = 239$ Wm^{-2}. Note that the astrophysical GE is much smaller than G_m^A . Among the authors, there seems to be an agreement that the absorption and re-emission of the surface upward infrared radiation by GHGs are the

principal causes for greenhouse warming. And, due to well established energy balance principles, increased atmospheric CO_2 concentration will be inevitably followed by an increased greenhouse effect. However, the fact is that the greenhouse effect is a differential quantity, therefore, such statements are not very well established and demonstrated. We have seen that G_m is a mixed quantity and cannot be associated with the net absorption of the S_U in the system.

The most popular global energy budget schemes were published by Kiehl and Trenberth (1997) (KT97), and TFK09. In KT97 and TFK09 the global average terrestrial radiation field was modeled by using a version of the US Standard Atmosphere 1976 (USST76) in which in order to match with Earth Radiation Budget Experiment, ERBE (2004) observations the H_2O column amount was reduced from 1.42 to 1.26 precipitable cm (prcm). In KT97 and TFK09 the all-sky G_m^A and clear sky G_m were reported as 155 and 157 Wm^{-2}, subsequently. Newer studies show substantially different greenhouse effects, see Stephens et al. (2012) (S12), Wild et al. (2013) (W13), and Costa and Shine (2012) (CS12). In Lacis et al. (2010) G_m^A is less by 5 Wm^{-2} than the one in RI06. The G_m in M10 shows about 10 Wm^{-2} underestimate, compared to the one in Lacis et al. (2010). Such differences in the radiative fluxes may be translated into about 1-2 K uncertainties in t_E and t_G temperatures. In Fig. 1, we show how CO_2 perturbations affect the OLR and how the real world responds to the changeing atmospheric CO_2 amount.

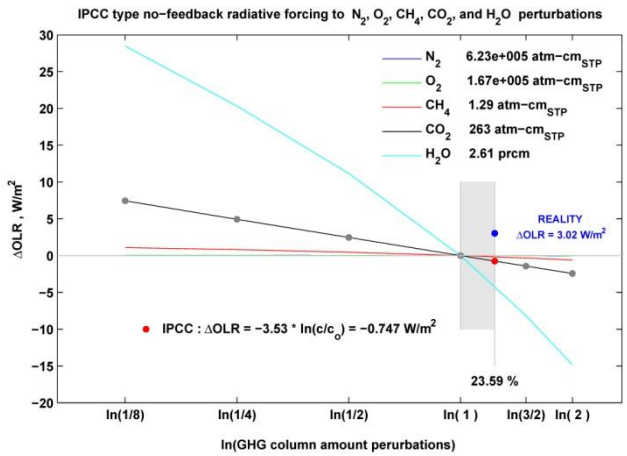

FIG. 1 HARTCODE GHG PERTURBATION STUDY SHOWS THAT AT THE TOA THE NO-FEEDBACK RESPONSE OF INCREASED ATMOSPHERIC CO_2 IS NEGATIVE. THE OBSERVED 23.6 % INCREASE IN THE CO_2 COLUMN AMOUNT CAUSES -0.75 WM^{-2} RADIATIVE IMBALANCE (RED DOT). IN THE SAME TIME PERIOD, BASED ON THE NOAA R1 ARCHIVE THE REAL CHANGE IS $\Delta OLR = 3.02$ WM^{-2} (BLUE DOT).

Climate modelers are using diverse - and not very transparent - H_2O feedback processes to match their predicted ΔOLR with the reality. Here ΔOLR is the difference between the OLR of the unperturbed and perturbed cases. In this article the High Resolution Atmospheric Radiative Transfer Code (HARTCODE) line-by-line (LBL) RT software are used for all flux computations. Typically, the spectral resolution was set to 1 cm^{-1}, Miskolczi (1989) .

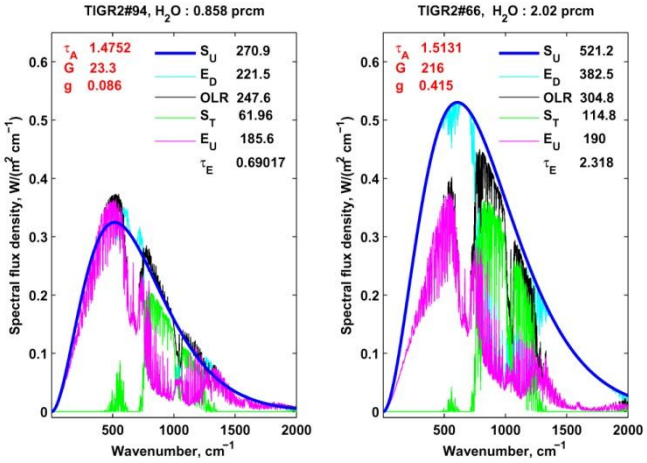

FIG. 2 SPECTRAL FLUX DENSITY COMPONENTS IN COLD AND DRY, (LEFT PLOT), AND WARM AND HUMID, (RIGHT PLOT), SITUATIONS. E_D : DOWNWARD ATMOSPHERIC EMITTANCE; G : CLEAR SKY GREENHOUSE EFFECT; τ_E : RADIATIVE EQUILIBRIUM FLUX OPTICAL THICKNESS. FLUXES ARE IN WM^{-2}.

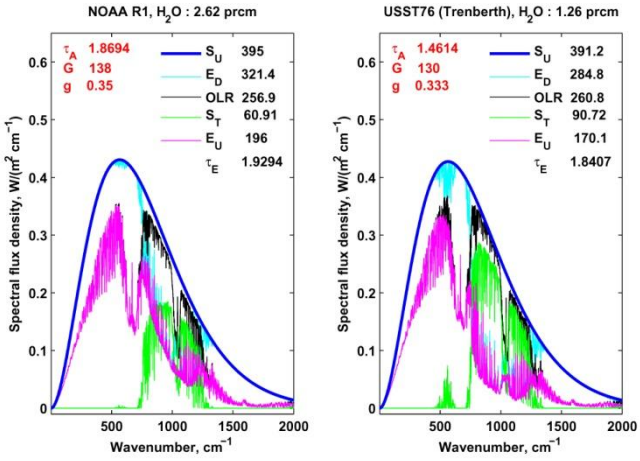

FIG. 3 SPECTRAL FLUX DENSITY COMPONENTS IN THE GLOBAL AVERAGE NOAA R1, (LEFT PLOT), AND USST76 , (RIGHT PLOT), ATMOSPHERES. FLUXES ARE IN WM^{-2} .

In Figs. 2 and 3 the theoretical difficulties of the interpretation of G as the measure of the absorption properties of the atmosphere have been demon-strated. In Fig. 2 local clear sky greenhouse effects are computed and compared for cold, and also for warm real atmospheric structures. The τ_A IR flux optical thicknesses are very similar in the two cases. The H_2O

column amounts and the radiative equilibrium optical thicknesses, τ_E, are largely different and are consistent with the H_2O amounts. Because of the chaotic nature of the humidity field and cloud cover, one cannot quantitatively relate the local G or g to the GHG content of the atmosphere.

In the second example (see Fig. 3) computations are performed using the 61 year global average atmosphere from the NOAA NCEP/NCAR (2008) reanalysis data time series (NOAA R1), and the version of USST76, used in KT97 and TFK09. Note that the H_2O column amounts in the two profiles are dramatically different. In the above example, the global average G and g are not sensitive to the roughly doubled water vapor amount in the atmosphere. These comparisons clearly show that the greenhouse effect characterized with G_m or G is not consistent with statements that link the increased GHG content of the atmosphere to increased IR absorption.

Considering the above examples, and the permanent failure of the most sophisticated general circulation models (GCMs) in predicting the magnitude of global warming, one should admit the serious theoretical deficiencies in using the greenhouse effect as a sole measure of infrared atmospheric absorption. The governing mechanisms of the IR absorption properties of the global average atmosphere are never studied in sufficient detail and the real nature of the greenhouse effect is not known. Compared to the observed ~0.012 K/year positive trend in the surface temperature over the last 61 years (see M10) and the recent skills of the GCMs in predicting the changes in the GE for a hypothetical CO_2 doubling, the quantitative proof of the CO_2 greenhouse effect based AGW is not imminent.

In any serious greenhouse study, the knowledge of the functional dependence of the global average IR flux optical thickness on the GHG concentrations, and the surface temperature, is absolutely necessary. The flux optical thickness, τ_A, flux absorption, A, and flux transmittance, T_A, are defined by the $S_T = S_U \exp(-\tau_A)$ and $S_T = S_U(1-A) = S_U T_A$ relationships. For semitransparent atmospheres, except in M04, M07 and M10, there are no published numerical data available on the theoretical surface temperature - flux optical thickness relationship. The obvious reason why the scientific community does not present such results is twofold.

The first is the lack of a suitable greenhouse theory which is based solely on the known fundamental laws of nature. Apart from the fact, that the use of GCMs for studying large scale climate change is conceptually wrong (fundamentally stochastic processes cannot be diagnosed by a deterministic model), the GCMs with their numerous tuning parameters are not representing the principles of physics and the demonstrated response of the greenhouse effect. Common greenhouse effect explanations are not able to account for the magnitude and the tendency of the phenomenon. It has been known for a long time that climate change is controlled by the net radiative fluxes at the TOA and at the ground surface. The global average state of the atmosphere (or global average climate) is governed by the laws that control flows of radiative fluxes at the boundaries.

The second reason is rather technical, and related to the accurate computation of the flux optical thickness. According to RI06 the three dimensional characterization of radiative heating rates from equator to pole using the LBL approach is impractical. This view suggests sacrificing accuracy, by using band models in global scale radiative transfer computations, where it is most needed. This simplified view is probably the reason why, in recent textbooks, extensive parts are devoted to popularizing ancient band model techniques, see for example in Pierrehumbert (2010). Unfortunately the fact is that there are no publicly available LBL codes for accurate computations of the IR flux optical thickness. From a correct LBL spectral radiance code there is a very long way to a correct spectral spherical refractive flux density code.

The IR Optical Thickness of the Atmosphere

In astrophysics - for the different kind of radiative transfer problems - there are different kinds of definitions for the mean optical thickness (or mean opacity), see Mihalas and Weibel-Mihalas (1999). They are the Rosseland, Planck, and Chandrasekhar means, and they are, in fact, different kinds of weighted average absorption coefficients. The relevant physical quantity necessary for the computation of the real atmospheric IR absorption is the Planck-weighted greenhouse-gas optical thickness, τ_A. The numerical computation of this quantity for a layered spherical refractive atmosphere may be found in M10. By definition, τ_A is computed from the spectral hemispheric transmittance and therefore represents the real spectral feature of the infrared absorption coefficient. It should be emphasized that τ_A is not a weighted absorption coefficient in the sense of the usual Planck

mean opacity in Mihalas and Weibel-Mihalas (1999). τ_A is a newly defined physical quantity and one cannot find any reference in the literature to its computational techniques. The existence of the large and organized absorption line catalogues and the development of high speed computers and LBL computational techniques are the reasons for the above definition of τ_A , see HITRAN2K (2002), Rodriguez et al. (1999). Only a full blown spherical refractive LBL radiative transfer code is able to compute the accurate atmospheric IR flux optical thickness. In short, τ_A may be expressed as:

$$\tau_A = -\ln\left[\frac{1}{\sigma t_G^4}\sum_{j=1}^{M}\pi B_\nu(\Delta\nu_j, t_G)\sum_{k=1}^{K} w^k \bar{T}_A(\Delta\nu_j, \mu^k)\right], \quad (1)$$

where $M = 3490$ is the total number of spectral intervals, $K = 9$ is the total number of streams, $B_\nu(\Delta\nu_j, t_G)$ is the mean spectral Planck function, and w^k is the hemispheric integration weight associated with the k^{th} direction (stream), $\bar{T}_A(\Delta\nu_j, \mu^k)$ is the directional mean spectral transmittance over a suitable short wave number interval:

$$\bar{T}_A(\Delta\nu_j, \mu^k) = \Delta\nu_j^{-1}\int_{\Delta\nu_j}\exp\left[-\sum_{l=1}^{L}\sum_{i=1}^{N}\left[c^{i,l} + k_\nu^{i,l}\right]\frac{u^{i,l}}{\mu^{l,k}}\right]d\nu \ , \ (2)$$

where $\mu^{l,k} = \cos(\theta^{l,k})/dz^l$ and $\theta^{l,k}$ is the local zenith angle of a path segment, $c^{i,l}$ and $k_\nu^{i,l}$ are the contributions to the total monochromatic absorption coefficient from the continuum type absorptions and all absorption lines relevant to the i^{th} absorber and l^{th} layer respectively. The vertical geometric layer thickness is dz^l . $N = 11$ is the total number of major absorbing molecular species and $L = 150$ is the total number of the homogeneous atmospheric layers (shells). In Eqn. (2) the wave number integration is performed numerically by fifth order Gaussian quadrature over a wave number mesh structure of variable length. At least $\Delta\nu_j \approx 1\,\text{cm}^{-1}$ spectral resolution is required for the accurate Planck weighting. From Eqn. (1) follows the usual form of the transmitted and absorbed part of the surface upward radiation. Eqs. (1,2) with the required spherical refractive ray-tracking algorithms are implemented into HARTCODE and facilitate the accurate partition of the OLR to its S_T and E_U components. The oversimplified and, in fact, often mathematically incorrect computation of G_m (for example in CS12, RI06, or in the NATURE article of Raval and Ramanathan (1989)) should be avoided.

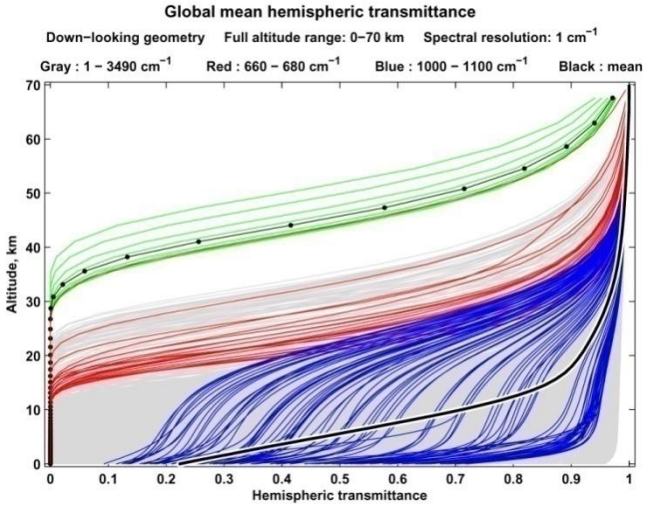

FIG. 4 DOWN-LOOKING CASE. HARTCODE SPECTRAL HEMISPHERIC TRANSMITTANCES IN THE 1-3490 CM-1 SPECTRAL INTERVAL FOR THE 668 CM-1 INTERVAL THE DIRECTIONAL TRANSMITTANCES ARE ALSO PLOTTED (WITH GREEN LINES). THE BLACK DOTS REPRESENT THE ISOTROPIC ANGLE AND INDICATE CONSIDERABLE ERROR IN THE WIDELY USED ISOTROPIC APPROXIMATION.

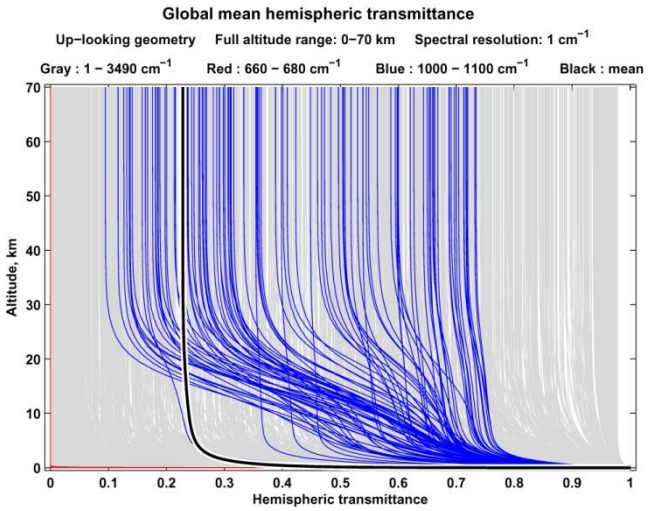

FIG. 5 HARTCODE SPECTRAL HEMISPHERIC TRANSMITTANCES IN THE 1-3490 CM-1 SPECTRAL INTERVAL. THESE TRANSMITTANCES ARE REQUIRED FOR THE COMPUTATION OF THE DOWNWARD FLUXES FROM THE TOA OR FROM THE CLOUD BOTTOM.

Unfortunately, theoretically, no instrument can be devised to measure the monochromatic or spectral S_T^ν and E_U^ν quantities separately. Since the above radiative components cannot be measured by any airborne or satellite spectrometer this is an essential improvement in the numerical computations of the real IR atmospheric absorption.

In Fig. 4 and Fig. 5 hemispheric transmittances (obtained from Eq. (2) by integration over the respective hemispheres) are presented for the global

average Thermodynamic Initial Guess Retrieval (GAT) profile and for down-looking and up-looking geometries. According to the Helmholtz reciprocity principle the spectral mean downward and upward hemispheric transmittances must be equal. In M10, page 234, the atmospheric transfer and greenhouse functions were introduced by the $f(\tau_A)=2/(1+\tau_A+T_A)$, and $g(\tau_A)=1-f(\tau_A)$ definitions. For an atmospheric air column in radiative equilibrium it was also shown that $f=OLR/S_U$, and $g=(S_U-OLR)/S_U$. Using the relationships above, the normalized greenhouse factor may be expressed with T_A, A, or τ_A. The complex, nonlinear dependence of g on the absorption properties of the atmosphere and the boundary layer fluxes is apparent. One must remember that the so called broadband window radiation is not an adequate quantity to represent the transmitted surface radiation.

To make use of the satellite measured global average broadband window radiation in global radiative budget estimates the data should be corrected (or calibrated) with global average atmospheric absorption data of the highest accuracy. Previously, in Fig. 3 accurate clear sky transmitted flux densities are presented for the GAT and the USST76 atmospheres. The 30 Wm^{-2} difference in S_T is large enough to raise the question of the quality of the KT97 and TFK09 global energy budgets. Although the USST76 atmosphere could be a good representation of an average mid-latitudinal atmospheric structure, the use of it in global energy budget assessments is a serious mistake.

It must be recognized that no consensus in global warming issues can exist without a declared and accepted standard global average atmosphere derived from a well documented global radiosonde archive. The total IR absorption of such an atmosphere must be computed for the most realistic chemical and GHG composition of the atmosphere and with the highest accuracy. All GHG studies and radiative budget estimates should be referenced to the absorption and optical properties of this global average standard atmosphere. In looking for flux density - optical thickness relationships, which could be used for surface skin temperature estimates, or in the quantitative computations of the GE sensitivities in GHG perturbation studies, such an atmosphere would be extremely beneficial. As an example, it has little merit to reference to RT computations where the atmospheric thermal and humidity structure (or the related input data base) are not traceable to the original sources. In the weakly documented low quality paper of CS12, no one knows how much water vapor or CO_2 is in the air, yet they suggest an accurate global average S_T for other people to use in their energy budget studies , see S12.

Although, in some cases, empirical estimates of radiative budget components from other authors are referenced, the critical evaluation of the different planetary radiative budget schemes is not the purpose of the present article. In general, in science, a debate over an issue is initiated when the related subject is sufficiently well known and both theoretical and empirical supports are available for the discussion. For example, no one will seriously comment upon the fictitious surface energy imbalance of 0.6 ± 17 Wm^{-2} in S12, or the 0.6 ± 0.4 Wm^{-2} in W13.

In the next sections we present numerical results of observed radiative flux density relationships for the planet Earth, identify and develop the theoretical relationships consistent with the observations and give a new view of the planetary greenhouse effect.

Input Data Sets

Realistic vertical global average thermal and humidity structures may be obtained from readily available climatological radiosonde archives, Chedin and Scott (1983). In this study the GAT global average structure is constructed from the Thermodynamic Initial Guess Retrieval (TIGR2) archive containing 1761 weather balloon observations. An updated version of the database (known as the TIGR2000 archive) containing 2311 soundings is also available: TIGR Thermodynamic Initial Guess Retrieval (2000). The locations, meridional, and annual distributions of the two archives are presented in Fig. 6. Both archives contain prohibitively large number of soundings for LBL computations.

One should be aware of some inconsistent and undocumented modifications of the vertical humidity structures in the TIGR2000 soundings. In hundreds of TIGR2000 observations the upper tropospheric humidity is significantly increased which may introduce biases in the computed global average vertical radiative structure. After some regional and seasonal grouping of the TIGR2 soundings a subset of 228 profiles is selected, see Fig. 7. In the subset the statistical characteristics of the original data set are preserved. In Fig. 8, two extreme atmospheric structures from the selected sub-set are presented.

In this article we use the GAT atmosphere as the representative temperature and humidity structures of the global average climate. For studying possible long term changes in the global average optical thickness (due to changes in GHG content of the atmosphere) the TIGR2 archive is not suitable. The publicly available longest time series of annual mean vertical temperature and humidity structures may be obtained from the NOAA R1 time series data archive. This archive, known as the NCEP/NCAR R1 data set, covers the 1948-2008 time period and is regularly updated. NOAA R1 has been used by the NCEP Climate Prediction Center to produce global atmospheric monitoring and assessment products, Trenberth (2009). A quick look at the data immediately shows that the range of variations in the annual mean over 61 years is very small: 58.87 atm-cm$_{STP}$ in CO_2, 0.0169 prcm in H_2O, and 0.687 K in surface temperature. The related year-to-year relative changes are also small, 0.35 %/year in CO_2, -0.0106 %/year in H_2O, and 0.0039 %/year in surface temperature. In this study monthly or seasonal variations are ignored.

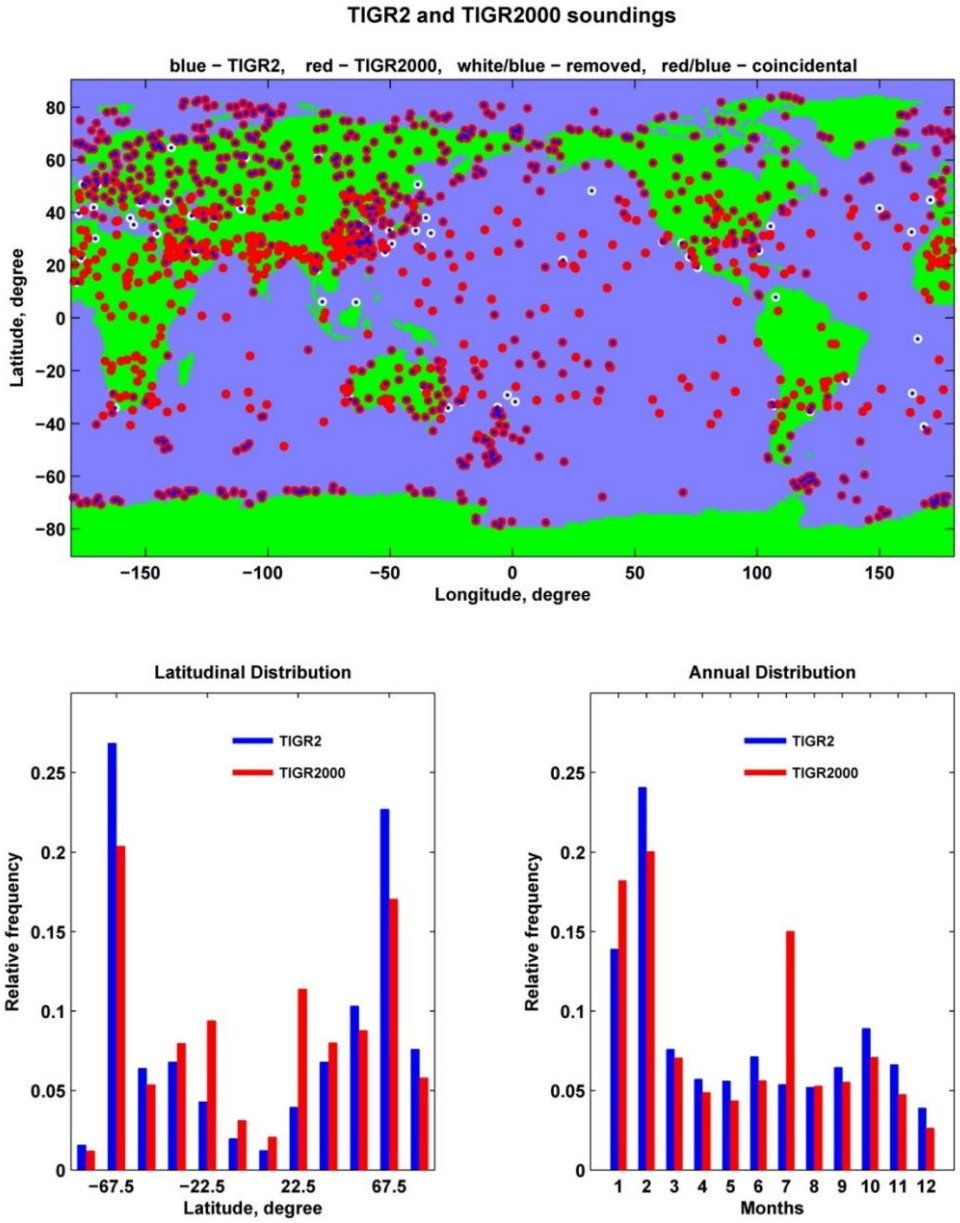

FIG. 6 THE TIGR CLIMATOLOGICAL DATASETS. DETAILED COMPARISONS SHOW THAT THE GLOBAL AVERAGE TIGR2 SURFACE AIR TEMPERATURE IS 0.28 K COLDER AND THE VERTICAL AIR COLUMN CONTAINS 0.1 PRCM (ABOUT 3 %) LESS H_2O. SINCE IN THE TIGR2000 VERSION THE VERTICAL H_2O STRUCTURE WAS ARTIFICIALLY MODIFIED (UPPER TROPOSPHERIC HUMIDITY WAS INCREASED) WE DECIDED TO USE THE ORIGINAL TIGR2 ARCHIVE.

Obviously, there are very high requirements for the sensitivity and numerical accuracy of the computed fluxes and flux optical thicknesses. To quantify the possible trend in the average absorption properties of the atmosphere, simulations are performed for six subsets of different times and time intervals.

Observed Empirical Facts

In 2002, at the National Atmospheric and Space Administration (NASA) Langley Research Center, the first set of global scale high accuracy LBL flux optical thickness and flux density computations for the TIGR2 data set were completed, and the new fundamental clear sky semi-transparent radiative equilibrium equation, $S_U(\tau_A) = OLR(\tau_A) / f(\tau_A)$, was awaiting large scale empirical verification. A general view of the simulated flux density components are presented as the function of the 11 seasonal and geographical classes in Fig. 9. A quick look at the upper plot immediately confirms the obviously expected relationships among the fluxes: $S_T < E_U < OLR < E_D < A_A < S_U$. The lower plot suggests a fairly strong linear relationship between the downward E_D and the absorbed A_A fluxes. After the routine plots of τ_A , T_A , S_U , S_T , E_D , E_U , and OLR quantities, four rather unusual relationships among the flux density components and optical thicknesses emerge. In Figs. 10-13 the TIGR2 simulation results are plotted for the individual soundings. The tentative naming of the discovered empirical relationships (they are called 'rules') reflects the fundamental physical laws with which they are associated. For completeness, we should also mention the extropy rule, which is not discussed here, see Miskolczi (2011).

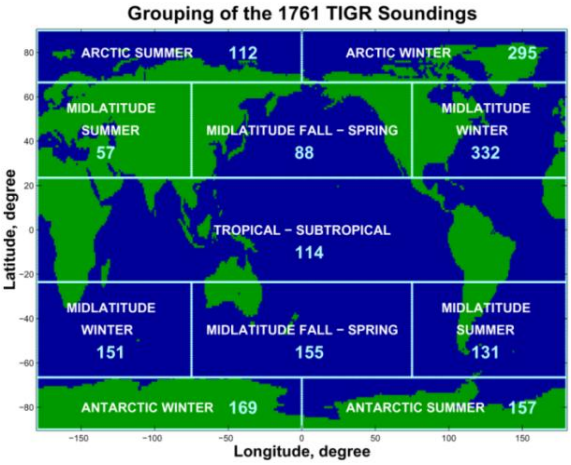

FIG. 7 LATITUDINAL AND SEASONAL GROUPING OF THE TIGR2 SOUNDINGS. IN THE SELECTED SUBSET 228 SOUNDINGS WERE DISTRIBUTED AMONG 11 GROUPS HAVING ABOUT 20 SOUNDINGS IN EACH GROUP. LATITUDINAL AND SEASONAL CLASSES WERE ESTAB- LISHED CONSIDERING THE SOLAR CLIMATIC ZONES.

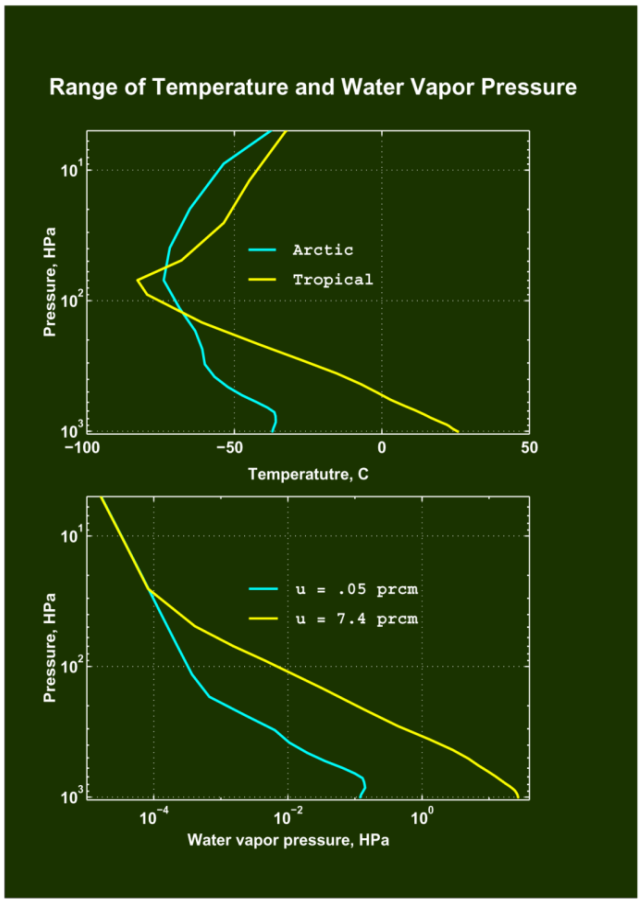

FIG. 8 RARE ATMOSPHERIC SITUATIONS. EXTREME DRY AND COLD AND WARM AND HUMID ATMOSPHERIC STRUCTURES IN THE TIGR2 DATA .

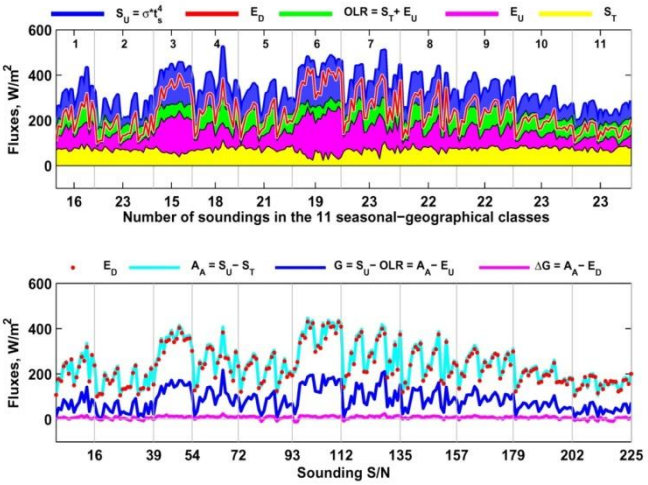

FIG. 9 SEASONAL-GEOGRAPHICAL DISTRIBUTIONS OF THE TIGR2 FLUX DENSITIES. CLASSES ARE: 1 - ARCTIC SUMMER, 2 - ARCTIC WINTER, 3 - NORTH MID-LATITUDE SUMMER, 4 - NORTH MID-LATITUDE FALL/SPRING, 5 - NORTH MID-LATITUDE WINTER, 6 - NORTH/SOUTH TROPICAL, 7 - SOUTH MID-LATITUDE SUMMER, 8 - SOUTH MID-LATITUDE FALL/SPRING, 9 - SOUTH MID-LATITUDE WINTER, 10 - ANTARCTIC SUMMER, 11 - ANTARCTIC WINTER. THE LOWER PLOT SHOWS THAT IN ALL CLASSES THE ATMOSPHERIC ABSORPTION CAN BE VERY WELL APPROXIMATED BY THE DOWNWARD ATMOSPHERIC EMISSION.

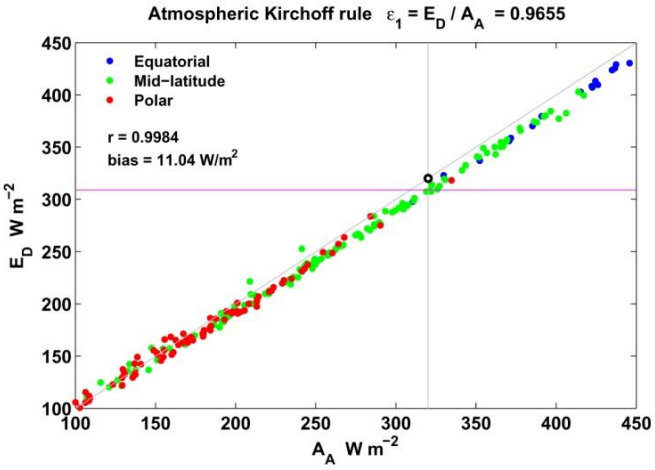

FIG. 10 THE ATMOSPHERIC KIRCHHOFF RULE SUGGESTS A VERY STRONG LINEAR RELATIONSHIP BETWEEN THE EMITTED CLEAR SKY DOWNWARD AND THE ABSORBED SURFACE UPWARD IR FLUX DENSITIES. COLD AND DRY POLAR AREAS FIT BETTER TO THE RULE THAN THE WARM AND HUMID EQUATORIAL AREAS. THE GLOBAL MEAN CLEAR SKY $E_D / A_A = \varepsilon_1$ RATIO (WE CALL IT SPHERICAL EMISSIVITY) IS ABOUT 3 %.

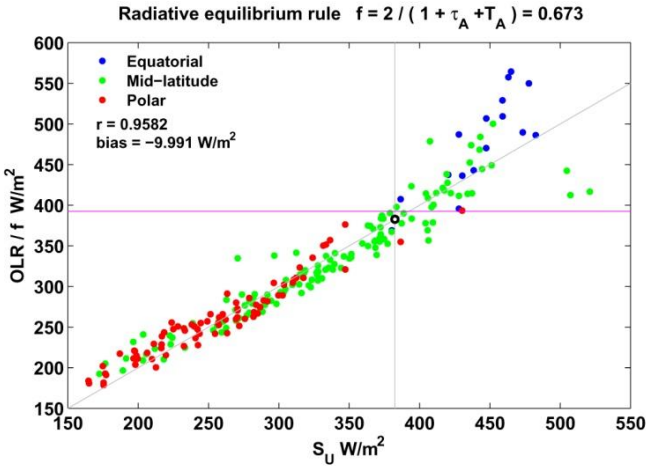

FIG. 11 THE RADIATIVE EQUILIBRIUM RULE IS THE NAME OF THE THEORETICALLY DERIVED $OLR / S_U = f$ EQUATION. FOR THE TIGR2 ARCHIVE THE GLOBAL AVERAGE TRANSFER FUNCTION IS SLIGHTLY LARGER THAN THE THEORETICALLY EXPECTED $f = 0.6618$. THE SCATTER OF THE POINTS SHOWS THAT THE EXACT LOCAL RADIATIVE EQUILIBRIUM IS A VERY RARE SITUATION.

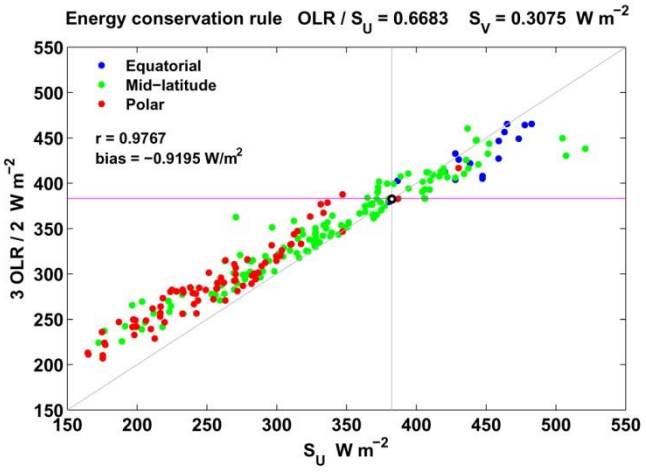

FIG. 12 THE $S_U = 3OLR / 2$ RELATIONSHIP SHOWS GOOD AGREEMENT BETWEEN THE GLOBAL MEAN (BLACK CIRCLE) AND THE THEORETICAL EXPECTATION (HORIZONTAL LINE). SINCE THE POLAR STATIONS OVERESTIMATE, AND THE EQUATORIAL STATIONS UNDERESTIMATE S_U THIS RELATIONSHIP IS ASSOCIATED WITH THE REDISTRIBUTION OF THE AVAILABLE THERMAL ENERGY OF THE ATMOSPHERE BY THE GENERAL CIRCULATION.

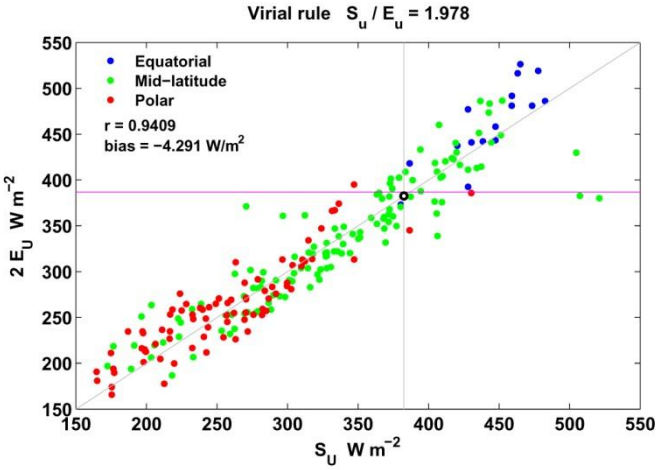

FIG. 13 THIS RULE IS THE RELATIONSHIP BETWEEN THE SURFACE UPWARD FLUX AND THE ATMOSPHERIC UPWARD IR EMISSION (EMERGENT THERMAL RADIATION FROM THE ATMOSPHERE ALONE): $S_U = 2E_U$. AGAIN WE HAVE A GOOD AGREEMENT BETWEEN THE GLOBAL AVERAGES. THIS RELATIONSHIP IS A DIRECT CONSEQUENCE OF THE GLOBAL AVERAGE HYDROSTATIC EQUILIBRIUM STATE .

At this point we should emphasize that the presented relationships are not derived from some well known physical laws of nature, but are obtained from observations and computations using first principles. It should also be noted that the newly discovered empirical relationships are not the results of some lucky coincidental profile selections from the TIGR2 archive. In the last several years the computations using the TIGR2000 archive, the updated NOAA R1 archive, some satellite training and calibration data sets, hundreds of high resolution and high quality radiosonde observations from the NOAA Testing and Evaluation Station are repeated. Many special atmospheric structures from different sources are evaluated as well.

No atmospheric structures contradicting the above rules are found. Even artificial profiles (like the USST76 atmosphere) are consistent with the new flux relationships. Judging from the correlation coefficients (Figs. 10-13), none of these rules are perfect. In fact, tight fits in these types of relationships are not

expected since the atmosphere is fundamentally a stochastic medium. We must conclude that the above rules represent the real radiative transfer properties of the Earth-atmosphere system, and in order to get closer to the cause of the greenhouse effect, one should try to explain and understand all of them.

Although this study focused on IR fluxes at upper and lower boundaries of the atmosphere, further results are presented in Fig. 14 for the GAT vertical radiative structure. Two sets of radiative fluxes (for the upper and lower portions of the atmosphere) are plotted as a function of the layer geometric thicknesses: $z(\Delta z) = z_{top} - z$, and $z(\Delta z) = z$, where $z_{top} = z_{70}$ is the 70 km top altitude of the atmosphere. The lower boundary of the whole air column is at $z_0 = 0$ km. For some selected altitudes numerical flux density data are presented in Table 1.

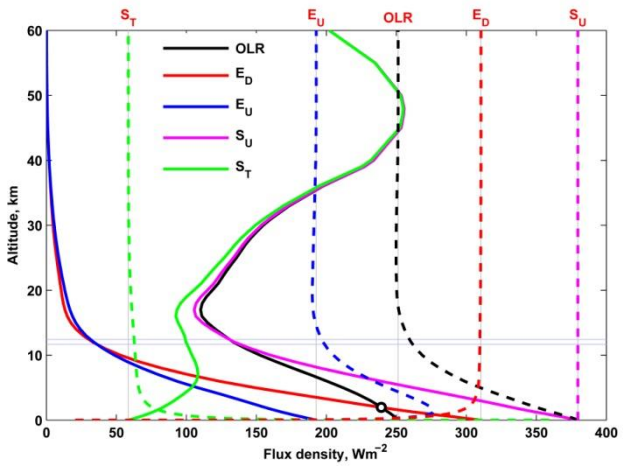

FIG. 14 GAT UPWARD AND DOWNWARD RADIATIVE FLUXES. SOLID LINES ARE THE BOUNDARY FLUXES FROM LAYERS BETWEEN z_{top} AND z ALTITUDES. BROKEN LINES ARE THE BOUNDARY FLUXES FROM LAYERS BETWEEN 0.0 AND z ALTITUDES. THE HORIZONTAL BLUE LINES ARE THE ALTITUDES WHERE $E_D(z) = E_U(z)$, AND $S_U(z) = OLR(z)$. AT THE ALTITUDE OF THE BLACK CIRCLE $E_D(z) = OLR(z)$.

The interesting features here are the approximate flux equalities at some special altitudes: $OLR(z_2) \approx E_D(z_2)$, $OLR(z_{10}) \approx B(z_{10})$, and $E_D(z_{10}) \approx E_U(z_{10})$. At the indicated levels the atmosphere has unique equilibrium states which may largely affect the whole global energy balance picture. For example, if the Kirchhoff rule is valid for all altitudes, then the $OLR(z_2) \approx E_D(z_2)$ equation means that, at around the 2 km altitude, the atmosphere above a cloud layer is in radiative equilibrium. The last two equations imply that slightly above the 10 km altitude the clear sky atmospheric greenhouse effect stops, $G = S_U - OLR = 0$.

The detailed analysis of the vertical structure of the IR radiation field will be the scope of another article. Note, that the NOAA R1 τ_A, and T_A are practically the same, but the lower atmospheric thermal structure of the GAT is considerably colder as there is an approximate 15 Wm^{-2} difference in S_U at the ground. This is a clear indication, that τ_A depends only upon the real absorption properties of the atmosphere.

TABLE 1. VERTICAL RADIATIVE STRUCTURE OF THE GAT ATMOSPHERE. ALTITUDES ARE IN KM, FLUXES ARE IN WM^{-2}, TRANSMITTANCES AND OPTICAL THICKNESSES ARE DIMENSIONLESS. THE NOAA R1 61 YEAR AVERAGE DATA ARE ALSO SHOWN IN RED COLOR. $B(z)$ IS THE FLUX DENSITY PROFILE AND $S_U = B_G = B(z = 0)$.

Altitude	*OLR*	E_D	E_U	$B(z)$	S_T	T_A	τ_A
60.0	**202.1**	**0.2008**	**0.1793**	**202.1**	**201.9**	**.9989**	**.0011**
50.0	**253.4**	**0.7421**	**0.6553**	**253.6**	**252.8**	**.9969**	**.0031**
30.0	**154.9**	**4.774**	**5.620**	**153.5**	**149.2**	**.9723**	**.0281**
15.0	**115.1**	**17.52**	**20.98**	**111.4**	**94.11**	**.8444**	**.1692**
10.0	**152.7**	**52.82**	**48.73**	**160.1**	**103.9**	**.6490**	**.4322**
5.00	**212.3**	**149.0**	**108.6**	**262.4**	**103.7**	**.3952**	**.9284**
2.00	**239.6**	**237.6**	**156.1**	**331.9**	**83.42**	**.2513**	**1.3810**
0.00	**251.8**	**309.9**	**193.2**	**379.7**	**58.6**	**.1542**	**1.8691**
0.00	**256.4**	**321.5**	**195.4**	**395.0**	**60.95**	**.1543**	**1.8688**

In the next three figures (Figs. 15-17) the results of the search for long term optical thickness trends in the 61 year long (1948-2008) NOAA NCEP/NCAR R1 re-analysis dataset are shown.

Attempts to identify any significant changes in the absorption characteristics of the atmosphere are unsuccessful. For the above tasks HARTCODE is pushed to extreme numerical accuracy, test runs for small GHG perturbations were presented in M10. In Fig. 15 the actual and expected atmospheric absorption trends are compared for the full time period. No change in the IR absorption is detected. In Fig. 16 the results of the six sub-sets of the 61 year time periods are also presented. The theoretical expectation in each sub-set is met, no changes in the sample mean optical thicknesses are apparent. However, both the annual mean optical thickness and H_2O column amount are subject to random fluctuations.

Detailed Fourier analysis of the 61 year long time series shows that a significant oscillation with a 3.529 year period is present in the data. This 'heartbeat' of the atmosphere could be related to the ElNino - LaNina cycles. Fig. 17 displays the observed changes in Δt_A, t_A, t_S, H_2O, and CO_2. The slight negative trend in Δt_A and the large increase in CO_2 concentrations is certainly not consistent with the classic GE explanations, found in any textbook on climate change.

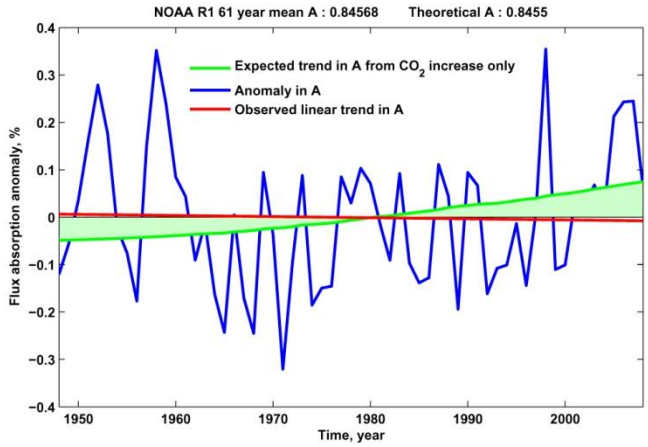

FIG. 15 ATMOSPHERIC ABSORPTION TRENDS IN THE LAST 61 YEARS. THE EXPECTED INCREASE IN THE ATMOSPHERIC FLUX ABSORPTION DUE TO THE ~23 % CO_2 INCREASE DURING THIS TIME PERIOD IS NOT PRESENT.

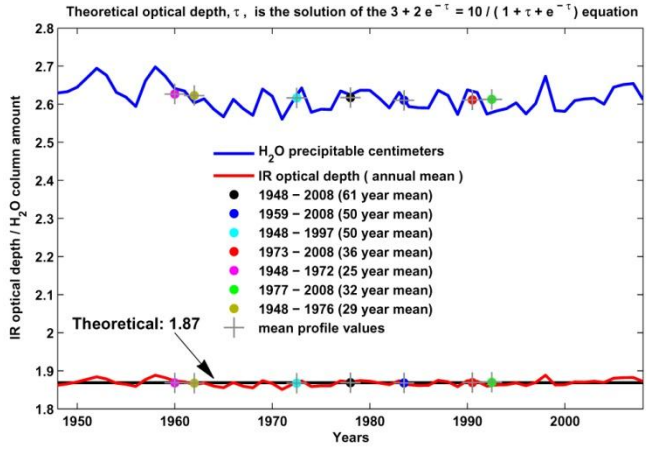

FIG. 16 OPTICAL THICKNESS COMPUTATIONS FOR DIFFERENT SUB-SETS OF THE NCEP/NCAR R1 ARCHIVE. SHORT TERM FLUCTUATIONS ARE NOT RELATED TO CO_2 INCREASE. THE AVERAGE τ_A IN ANY TIME SERIES AGREED WITH THE THEORETICAL EXPECTATION OF 1.87 .

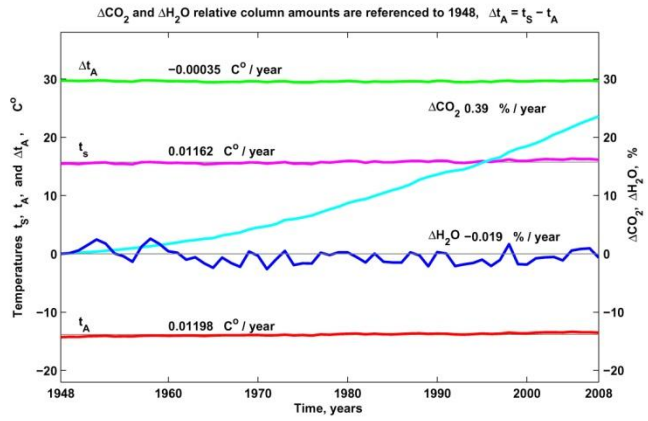

FIG. 17 THE OBSERVED GREENHOUSE TEMPERATURE CHANGE IS NOT CONSISTENT WITH THE INCREASED CO_2 CONCENTRATION. THE SURPRISING STABILITY OF Δt_A CANNOT BE EXPLAINED BY THE CLASSIC VIEW OF GREENHOUSE PHENOMENON, AND DOES NOT SUPPORT THE GE BASED AGW HYPOTHESIS OF THE IPCC.

Theoretical Interpretations

The analytical equations of the presented rules in Figs. 10-13 are summarized in the next four equations:

$$E_D = A_A = S_U A = S_U (1 - T_A) , \quad (3)$$

$$OLR / S_U = f , \quad (4)$$

$$S_U = 3OLR / 2 , \quad (5)$$

$$S_U = 2E_U . \quad (6)$$

In the range of the input data sets the atmospheric Kirchhoff , radiative equilibrium, and virial rules, Eqs. (3,4) appear to be valid for each individual sounding and also for the global averages. The energy conservation rule and virial rule, Eqs. (5,6) are valid for only the global averages. Although in M07 some successful modelling and simulation results for the Martian atmosphere have been published, the validity of Eqs. (3-6) for other planets are not discussed here. Each planet or moon in the solar system has its own distinct physical condition and in each case the radiative transfer problem must be formulated individually.

Atmospheric Kirchhoff Rule

Recently some researchers have raised the question of the applicability of the Kirchhoff rule for atmospheric radiative processes, see for example DeBruin (2010), Spencer (2011). Since the atmospheric Kirchhoff rule represents an empirical fact, such critiques do not have much scientific ground. If a couple of hundred atmospheric structures show the $E_D \approx A_A$ approximate equality, then the only way to refute this relationship is to show an atmospheric structure which is violating it. In a planetary radiative equilibrium situation the strict $E_D = A_A$ relationship at the lower boundary is established with the material IR emissivity properties of the ground surface and atmosphere.

The anisotropy in E_D and the IR emissivity (or reflectance) of the ground surface cannot be ignored. The different forms of the monochromatic, flux, directional etc., Kirchhoff laws are well known in the general radiative transfer theory. It is also known that the classic monochromatic Kirchhoff law is not valid in the close vicinity of strong absorption/emission lines, see M07. It is also difficult to adopt this law for atmospheric IR flux densities where the inhomogeneous atmosphere is in permanent physical contact with solid and liquid surfaces. The important finding here is the ability of any real atmosphere to instantly adjust its radiative structure to closely satisfy Eq. (3).

The physical explanation is very simple. The relaxation time of the IR radiation field is much smaller than any macroscopic heat or energy transfer processes (related to the motion and thermodynamics) of the atmosphere. The vibrational-rotational relaxation time is in the order from 2×10^{-6} to 2×10^{-5} sec at 1 atm. and 200K. The IR radiation field is close to quasi-static equilibrium with the surrounding environment and it instantly 'sees' the whole atmosphere, independently of the dynamics of the system. The strict validity of the spectral Kirchhoff law for a hypothetical isothermal atmosphere is obvious. Such computation is presented in Fig. 18. As can be concluded, the spectral Kirchhoff law is exact, and perfectly reproduced, (see the red line). Similar but spectral radiance simulations for isothermal atmospheres are routinely performed to test the numerical performance of LBL radiative transfer codes, see Kratz et al. (2005). The computational (numerical) accuracy of our LBL code for flux transmittance is excellent. The relative error in the $E_D = A_A$ equality is $100(1-E_D/A_A) = 2.2\times10^{-6}$ %.

The conditions of the stability of the thermal structure of an air column are also of interest. In Figs. 19 and 20 simulated global average flux transmittance, atmospheric downward emittance, and observed source function profiles are presented for clear and cloudy GAT atmospheres. In these simulations the cloud layer is represented by a perfect black surface at a given altitude with an infinitesimal vertical extension and in thermal equilibrium with the surrounding air. The thermal equilibrium and a perfectly black radiator are also assumed at the ground surface, $S_U = \pi B(z_0)$ at zero altitude. In Fig. 19 the whole atmospheric air column is in radiative equilibrium with the surface air. This is the obvious condition for the local thermodynamic equilibrium (LTE), and the existence of a stable temperature profile. At higher altitudes this figure shows that any emitting cloud layer is also in radiative equilibrium with the atmospheric column above. This is also the condition of the LTE in the air column above the cloud layer. We should note that in case the global average atmosphere represents a long term average structure which is in overall radiative balance with the surrounding space, then the ~3 % global average anisotropy effect in the Kirchhoff rule must be accounted for by an effective spherical emissivity factor of $\varepsilon_1 = 0.9652$. In Fig. 20 the cloud layer is acting as a cavity and the atmosphere below the cloud layer is in radiative equilibrium with the emitting surfaces at the upper and lower boundaries.

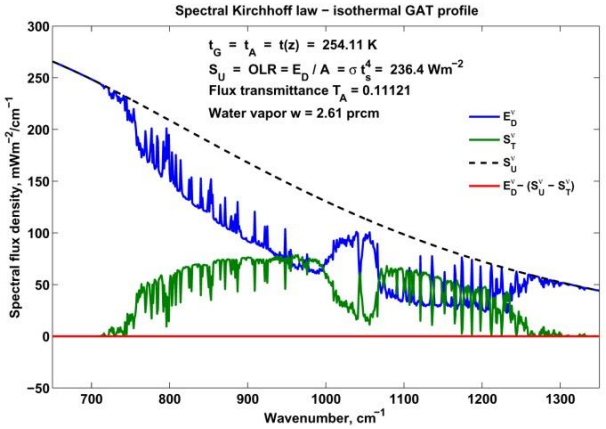

FIG. 18 THE SPECTRAL KIRCHHOFF LAW IN ISOTHERMAL ATMOSPHERE REQUIRES THE FOLLOWING EQUALITIES: $OLR = S_U = E_D / A = E_U / A$, AND $E_U / S_U = E_D / S_U = A$. THE $S_U = OLR / f$ AND $S_U = E_D / A$ EQUATIONS CANNOT BE SATISFIED SIMULTANEOUSLY, THEREFORE, SEMI-TRANSPARENT ISOTHERMAL ATMOSPHERE CANNOT BE IN RADIATIVE EQUILIBRIUM.

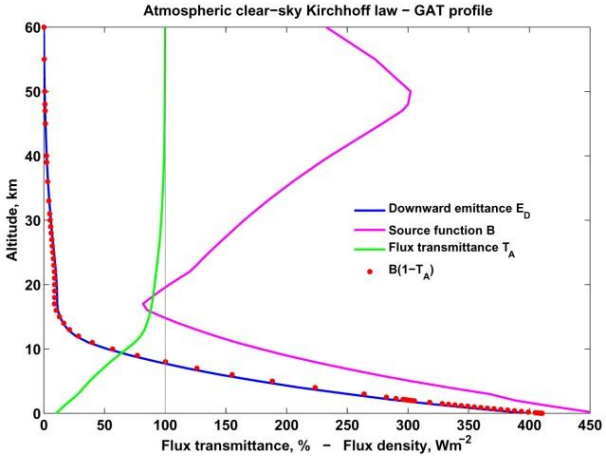

FIG. 19 CLEAR SKY KIRCHHOFF LAW. THE ATMOSPHERIC DOWNWARD EMITTANCE IS EQUAL TO THE ATMOSPHERIC ABSORPTION OF THE SURFACE UPWARD RADIATION.

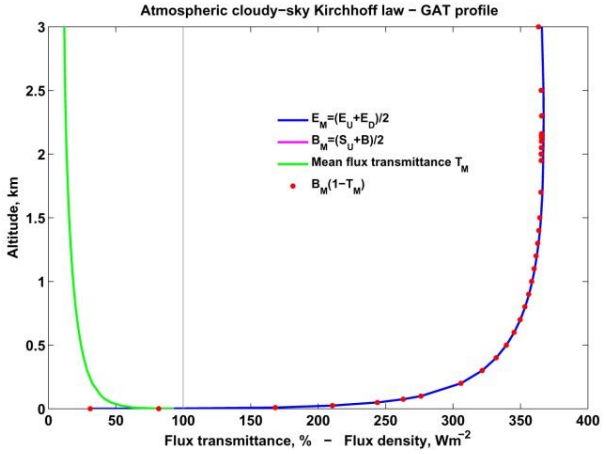

FIG. 20 CLOUDY SKY KIRCHHOFF LAW. UP TO ABOUT 3 KM ALTITUDE THE MEAN ATMOSPHERIC EMITTANCE IS EQUAL TO THE ABSORBED MEAN SURFACE RADIATION (FROM GROUND AND CLOUD BOTTOM), T_M IS THE WEIGHTED AVERAGE FLUX TRANSMITTANCE.

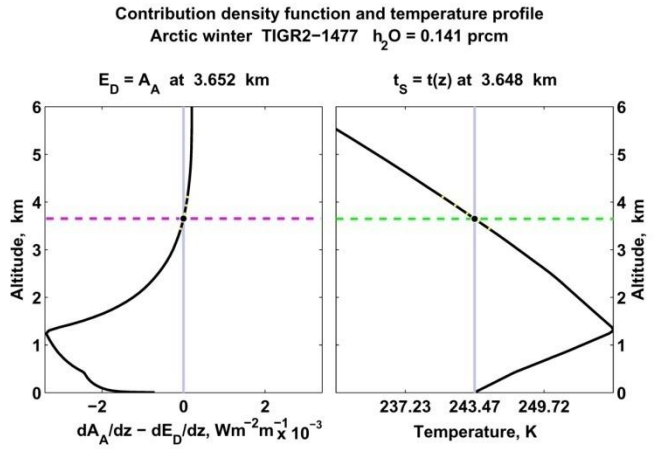

FIG. 21 LOW LEVEL TEMPERATURE INVERSION AND RADIATIVE EXCHANGE EQUILIBRIUM. HARTCODE DETERMINED THE EQUILIBRIUM ALTITUDE USING THE YELLOW DOTS FOR INTERPOLATION. THE ACCURACY OF THE EQUILIBRIUM ALTITUDE IS ~ 4 M.

The question of the radiative exchange equilibrium (introduced in M10) between the surface and a particular part of the atmosphere is also studied. In case thermal inversions are present in the temperature profile, theoretically the surface must be in perfect radiative exchange equilibrium with those atmospheric layers having the same temperature. For this kind of computation 42 inversion cases are selected from the TIGR2 data and the differences in the absorbed and emitted radiations in each layer are computed. Such kind of tests are very useful because they can point to inconsistencies and programming bugs in the computational algorithms.

In Fig. 21, results are presented for a cold and dry arctic atmosphere showing ~5 K close-to-surface temperature inversion. The return altitude of the temperature profile (above the inversion layer) is picked up with quite remarkable accuracy (~ 4 m). To our satisfaction, HARTCODE computed the layer net radiation according to our expectations. As we mentioned already, the IR radiative imbalance at the ground surface can easily be accounted for by introducing material IR emission properties of the atmosphere and the surface. The complete radiative equilibrium at the surface can be, and must be established.

Radiative Equilibrium Rule

The naming of "radiative equilibrium rule" is quite straightforward. The new semi-transparent radiative equilibrium equations, the derivation Eq. 4 from well known principles of the general radiative transfer theory are proved with sufficient mathematical rigor, (see Appendix B, Eq. B8 in M07). However, the use of radiation equilibrium terminology requires some clarification. The definition of the piecewise radiative equilibrium is given by $B(\bar{\tau}) = (3/4\pi)H\bar{\tau} + B_o$, where $B(\bar{\tau})$ is the source function profile, H is the Eddington flux, B_0 is an integration constant, and $\bar{\tau}$ is the average flux optical depth (measured from the TOA). In our terminology, once a linear (actual or equivalent) source function profile is established with the required slope and $B_0(\bar{\tau}_A)$, then the atmosphere is said to be in radiative equilibrium. In this case the atmosphere has the required amount of GHGs (H_2O, CO_2, O_3 etc.) to support the $S_U = OLR/f$ relationship. An equivalent form of Eq. (4) may be obtained using the $E_U + S_T = OLR$ defining identity: $S_U = E_U/(f - T_A)$.

It is important to note, that at the theoretical derivation in M07 the gray approximation is just a simplified terminology and applied only for the convenience of dropping the wave number index in the equations. In case of monochromatic radiative equilibrium, one may rewrite the solution in the monochromatic form: $f^\nu S_U^\nu = OLR^\nu$, where $f^\nu = f^\nu(\tau_A^\nu)$ and τ_A^ν are the monochromatic transfer function, and the monochromatic flux optical thickness respectively. Integrating both sides with respect to the wave number and applying the mean value theorem of the calculus one may easily arrive at Eq. (4).

In 2002 the only available theoretical relationship between the IR optical thickness and the source function profile was the classic semi-infinite Eddington solution, and its corrected versions (which tried to resolve the surface temperature discontinuity problem). However, the related equations for semi-transparent atmospheres turned out to be mathematically incorrect and should not be used. In a real global average clear sky atmosphere where the net non-radiative energy fluxes equal to zero Eq. (4) holds exactly.

The global average TIGR2 atmosphere used in this article is quite close to the state of radiative equilibrium. Test runs in the 0-120 km altitude range show that S_U = 379.688 Wm^{-2}, $OLR = 251.004$ Wm^{-2}, $f = 0.661144$, and the error in Eq. (4) is negligible, $S_U - OLR/f$ = 0.037 Wm^{-2}. Because of the changes in OLR and f, reducing the altitude range to 0-70 km, Eq. (4) will overestimate S_U by about ~1 Wm^{-2}, but will largely reduce the LBL computational burden.

Energy Conservation Rule

Before going into the details of the physical meanings of the rules presented in Figs. 12 and 13, we should spend some more time with the energy conservation and virial rules. In these two rules the clear sky surface upward flux is proportional with OLR and also, with E_U : $S_U = 3OLR/2$ and $S_U = 2E_U$. Unfortunately these equations do not satisfy an obvious and necessary physical condition which is sometimes called the transparent limit constraint.

For a transparent atmosphere, $\tau_A = 0$, $S_U = S_T = OLR$, and $E_D = E_U = 0$ conditions should be satisfied. To implement the transparent limit constraint the $S_V = S_T/2 - E_D/10$ virial term is introduced. Adding S_V to the left hand side of Eq. (5), an equation which obeys the transparent limit, and satisfies both of the original equations is obtained. It is easy to show that Eqs. (5) and (6) can be trivially satisfied with $S_T/S_U = 1/6 : S_U = 2E_U = 2OLR - 2S_T = 2(2S_U/3) - 2S_T$, from which follows $S_U = 6S_T$. The equivalent form of this equation (using the observed $E_D = A_A$ approximation) is $S_T - E_D/5 = 0$. It is assumed that the general equation should be in the form of $S_U + S_V = 3OLR/2$, where $S_V = X(S_T - 5E_D)$ and X is a non-zero multiplier. In the transparent atmosphere limit $S_U + X\,S_U = 3S_U/2$, from which $X = 1/2$, and $S_V = S_T/2 - E_D/10$. The final form is $S_U + S_T/2 - E_D/10 = 3OLR/2$ which can be reshaped into a much simpler form:

$$S_U = OLR/(3/5 + 2T_A/5) \ . \qquad (7)$$

From Eq. (7) and the definition of OLR the $5/3 = A_A/E_U$ simple relation and the $5/3 \approx E_D/E_U$ approximation immediately follow. One should not forget, that Eq. (7) (and its different forms) are applicable only for global average atmospheres. For example, the A_A/E_U ratios for the TIGR2 and USST76 atmospheres are 1.666, and 1.766 subsequently, (see Fig. 3). $S_U = 3OLR/2$ requires the validity of $E_D = A_A$. This follows directly from the greenhouse identity, which expresses the conservation of the radiant energy. Applying the $E_D \approx A_A$ approximation one arrives at the $S_U - OLR \approx E_D - E_U$ equation, from which one may readily obtain the $S_U \approx 3OLR/2$ relation. In complete planetary radiative equilibrium $E_D = A_A$, and $S_U = 3OLR/2$. The violation of these rules leads to the violation of the conservation of radiant energy as explained in M07 Eq. (7) in page 7.

Virial Rule

Climate scientists tend to forget about the virial theorem and they usually render it unusable for climate research. The atmospheric virial rule, $S_U = 2E_U$, shows a linear dependence between the surface upward flux density and atmospheric upward emittance. Under hydrostatic balance the virial theorem relates the potential energy and the internal energy. The virial theorem may be expressed in different forms : $2T + \Omega = 0$, or $3(\gamma - 1)U + \Omega = 0$, where T is the mean kinetic energy, Ω is the gravitational potential energy, γ is the specific heat ratio and U is the internal energy of the system, see Chandrasekhar (2010), Cox and Giuli (1968) and Clausius (1870). In astrophysics the Vogt-Russel theorem is a relationship between the mass and luminosity of a star.

The above facts gave enough inspiration to try to relate E_U to the surface pressure or to the mass of the atmosphere. The computations for the TIGR2 archive are presented in Fig. 22. It is quite obvious that the virial theorem is applicable for the Earth's atmosphere and represents a permanent constraint on the IR radiation field. For the Earth atmosphere the differential forms of the virial relationship is also confirmed quantitatively (not shwn here).

The critiques of the association of Eqs. (6) with the virial concept in DeBruin (2010), Toth (2010), and in the comments of other radiative transfer experts (see E. Rabett, P. DeWitt, G. Schmidt, R. Pierrehumbert, and B. Levenson in the Real Climate (2008), or Science of Doom (2014) Blogs) have no theoretical and empirical foundations.

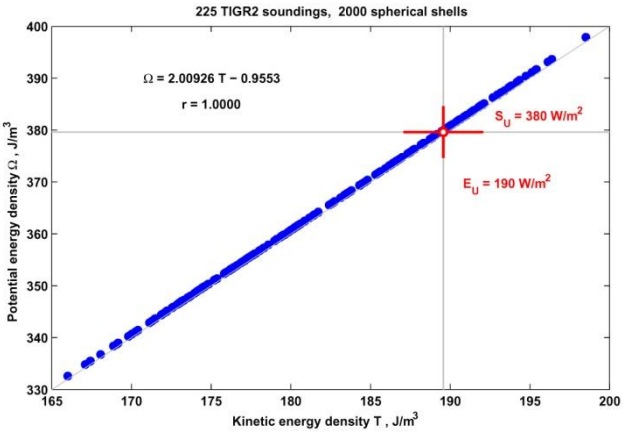

FIG. 22 VIRIAL CONCEPT IN HYDROSTATIC ATMOSPHERE. INTERNAL ENERGY IS COMPUTED WITH ONE DEGREE OF FREEDOM. GRAVITATIONAL POTENTIAL ENERGY DENSITY IS REFERENCED TO THE SURFACE.

Results and Discussion

As soon as sufficient confidence in the validity of the individual clear sky atmospheric radiative transfer rules is gained, the author is facing the interesting problem of the empirically proven constant global average clear sky flux optical thickness. Obviously the energy conservation and radiative equilibrium rules are the relevant equations which may be associated with the overall planetary radiative balance and give the needed theoretical support.

The simultaneous validity of Eqs. (4,7) requires the solution of the $OLR/(3/5+2T_A/5)=OLR/f$ transcendental equation which can be simplified into the $g=2A/5$ form. The only unknown in these equations is the equilibrium flux optical thickness which is the sole function of the thermal and humidity structure of the global average atmosphere.

The numerical solution of the equation resulted in a unique theoretical equilibrium flux optical thickness of $\tau_A^T=1.867561$. The other theoretical quantities are derived from τ_A^T :$T_A^T=0.1545$, $A^T=0.8455$, $f^T=0.6618$, $g^T=0.3382$. $\varepsilon_1^T=0.9572$. Apparently this τ_A^T does not depend on any particular GHG concentration and it might better be regarded as an invariant climate parameter of the Earth-atmosphere system.

The first verification of the $\bar{\tau}_A=\tau_A^T$ equality is based upon the TIGR2 and NOAA R1 radiosonde archives ($\bar{\tau}_A$ is the observed global average). The combined results are summarized in Fig. 23. All annual global mean optical thicknesses are practically equal to τ_A^T and supporting the $\bar{\tau}_A=\tau_A^T$ theoretical expectation. Fig. 23 shows also the TIGR2 E_U/S_U ratios (gray dots) and the associated theoretical $f-T_A$ function (magenta curve).

One should note that despite the relatively large spread of the E_U/S_U dots, the global average $\bar{E}_U/\bar{S}_U=0.5089$ ratio is consistent with the $\bar{S}_U=2\bar{E}_U$ virial rule. In our atmosphere the individual E_U/S_U ratios are also constrained by the T_A, A, f, and g radiative transfer functions (see the yellow shaded area). The theoretical upper limit of τ_A is set by the $f=g=1/2$ constraint: $\tau_A^{max}=2.9475$. The $1-2A/5$ (broken red curve) is a version of the energy conservation rule, and the green dot in the intercept of the f and $1-2A/5$ curves marks the position of τ_A^T.

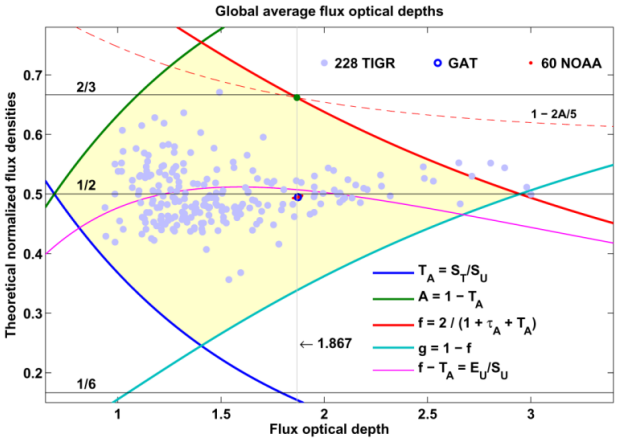

FIG. 23 COMBINED TIGR 2 AND NOAA SIMULATIONS. THE ANNUAL MEAN NOAA R1 DATA NOT RESOLVED SUFFICIENTLY TO SEE THE INDIVIDUAL SOUNDINGS. THE EMPIRICAL $\bar{\tau}_A=\tau_A^T=1.87$ RELATION SHIP IS FULLY SUPPORTED.

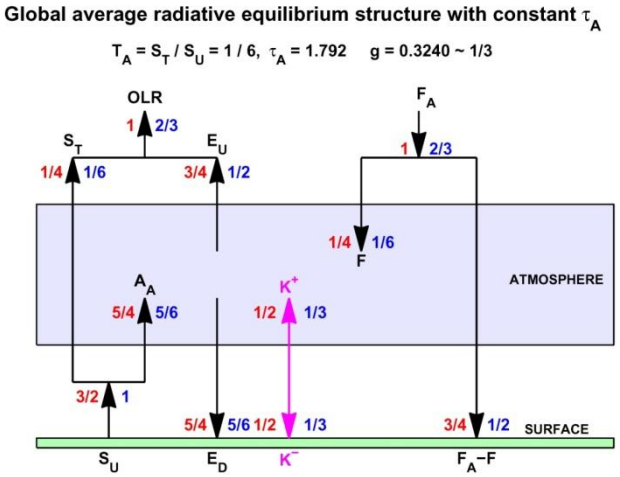

FIG. 24 STEADY-STATE CLEAR SKY CLIMATE MODEL WITH CONSTANT IR OPTICAL THICKNESS. RED NUMBERS: $OLR=1$; BLUE NUMBERS: $S_U=1$. IN RADIATIVE EQUILIBRIUM $S_U=F_A/f$, AND $S_U=F_E(1-\alpha_B)/f$, THEREFORE, S_U MAY CHANGE ONLY THROUGH F_E OR α_B.

The observed stability of the clear sky absorption properties of the global average atmosphere may be demonstrated with a heuristic clear sky RT model presented in Fig. 24 (here F is the absorbed part of F_A within the atmosphere). This model is simplified in a sense that the effects of the LW emissivity, reflectance,and anisotropy are ignored on the basis the sustained radiative equilibrium requirement will compensate all related imbalances. The net non-radiative processes $K^+ + K^-$ are zeroed out on the basis, that the planet is in radiative equilibrium and the hydrological sub-system (or water cycle) is a closed equilibrium process. The only requirement from the model is the constant average IR optical thickness which can be maintained around the τ_A^T theoretical

value by the stochastic fluctuations of all flux density ratios (around their respective planetary averages). Compared to the real world relationships among the boundary fluxes in Table 1, this model gives quite a reasonable estimate of the normalized flux densities.

The constant long term global average clear sky flux optical thickness does not leave much room for the system to obey the energy conservation principle. It is quite plausible to assume that the cloud cover is responsible for simultaneously maintaining the radiative equilibrium and energy conservation requirements. Some aspects of the global average cloud cover will be discussed in the next section, but the full account of the detailed role of the hydrological cycle and its quantitative effect on the flux density components will be discussed elsewhere.

Radiative Equilibrium Cloud Cover

One of the most elusive problems of climate science is the correct handling of the radiative effects of the global average cloud cover. After decades of struggle with the cloud forcing parameter and other mixed physical quantities, the role of clouds in the climate system remains hidden. It has been known for a long time that the cloud cover follows the annual solar cycle which is present in the SW energy input ($330.25 < F_E < 353.00$ Wm^{-2}), but a solid theoretical foundation for the mechanism and the quantitative methods for the practical evaluation of the β and h^C parameters are not present in climate literature.

Accurate RT computations using HARTCODE lead to the discovery of four fundamental atmospheric radiative transfer rules. As an application, in this section the radiative equilibrium β, and h^C which are consistent with the above rules and the related constraints are determined. In view of the $\overline{\tau}_A = \tau_A^T$ and $OLR = S_U f(\tau_A^T)$ clear sky LW radiative equilibrium requirements it is obvious, that the task of assuring the all-sky radiative balance and the $OLR^A = F_E - F_R$ top level energy conservation constraint, is left entirely to the β, and h^C parameters.

We should mention, that in M07 an attempt is already made to compute β, and h^C from the atmospheric Kirchhoff, and the energy conservation rules: $\beta = (S_U - 3OLR^A / 2) / (S_U - S_U^C)$, where $S_U = 382$ Wm^{-2}, $OLR^A = 235$ Wm^{-2}, and $S_U^C = 333$ Wm^{-2}. The resulted $\beta = 0.6$ and the related $h^C = 2.05$ km cloud top altitude fit well into the wide range of published cloud cover data, but unfortunately, large uncertainties in the satellite OLR^A may result in any β within the $0.45 < \beta < 0.75$ range. Because of the $OLR^A \approx OLR^C$ assumption and the limited capability of the HARTCODE vertical layering routines (at that time), the accuracy of our β and h^C was unknown. It was impossible to prove the consequential $A_A^C(h^C) = OLR$, $\beta = f(\tau_A^T)$, and $E_D(h^C) = OLR^C$ relationships from the Kirchhoff rule (see page 19 in M07).

In the recent approach it is assumed that the GAT atmosphere represents the global average structure reasonably well, and the F_0, (and consequently F_E), are also known with sufficient accuracy. One may construct two discrete sets of data ($\beta^A(\alpha_B, h^C)$, and $\beta^E(\alpha_B, h^C)$) from LBL simulations of the OLR^A, OLR, and OLR^C flux densities:

$$\beta^A = ((1-\alpha_B) S_E - OLR) / (OLR^C(h^C) - OLR), \quad (8)$$

$$\beta^E = (OLR^A / (1-\alpha_B) - S_U) / (S_U^C(h^C) - S_U). \quad (9)$$

$\beta^A(\alpha_B, h^C)$ and $\beta^E(\alpha_B, h^C)$ are the cloud fractions from the $\beta^A OLR^C + (1-\beta^A) OLR = F_A$ and $\beta^E S_U^C + (1-\beta^E) S_U = F_E$ equations, respectively. Note that in spherical geometry the cloud fraction does not depend on the altitude. In the two-dimensional optimization problem, only one global average cloud layer is assumed and the $\| \beta^A - \beta^E \|^2$ norm is minimized. For obtaining accurate β, and α_B, the vertical resolution of the HARTCODE altitude vector is set to 40 cm.

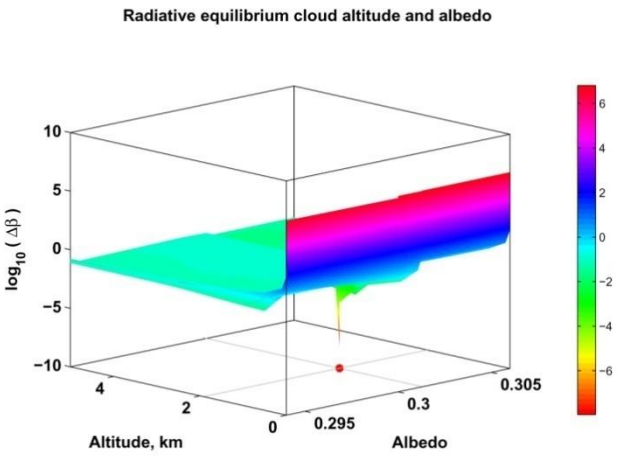

FIG. 25 RESULTS OF THE MULTIVARIABLE NONLINEAR OPTIMIZATION. THE EQUILIBRIUM CLOUD COVER, BOND ALBEDO, AND CLOUD TOP ALTITUDE ARE $\beta^T = f(\tau_A^T) = 0.6618$, $\alpha_B = G_E = 0.3013$, AND $h^C = 1.9160$ KM.

The range of α_B is not that critical, here the solution somewhere between $0.294 < \alpha_B < 0.306$ is expected. In Fig. 25 the three-dimensional view of the optimization results are shown. In the close vicinity of the minimum, the norm changes 2-3 orders of magnitude, indicating a very sharp extremum. The results show extremely good numerical agreement between β^T and f^T: $\beta^T = f(\tau_A^T) = 0.6618 \pm 10^{-7}$.

The equilibrium albedo and cloud top altitude are: $\alpha_B = 0.301290611$, and $h^C = 1.9160$ km, respectively. Some other ways of finding the accurate β, and h^C have been presented in Miskolczi (2014).

The independent empirical global average cloud cover estimates from the ISCCP are consistent with our results. From a 20 year long time series (ISCCP−D2 198307−200806 in Van Andel (2010)) a global mean β of 66.38 +/− 1.48 % was reported. The 10 year average ISCCP data show similar global cloud cover, $\beta = 66$ %, Ollila (2013).

According to the $E_D^A = g\,E_D + f\,OLR^{Cd}$ relationship the LW back radiation (through the OLR^{Cd} term) depends on the cloud altitude. Using our equilibrium transfer function f^T and h^C the back radiation is $E_D^A = 345.98$ Wm^{-2}. This value is quite consistent with the observed $E_D^A = 345.4$ Wm^{-2} (ISCCP-FD value for the CERES period from March 2000 to May 2004), see Table 2 in TFK09, and the $E_D^A = 345.6 \pm 9$ Wm^{-2} quoted by S12 in their NATURE article. W13 gives the best estimate of the back radiation as $E_D^A = 342 \pm 5$ Wm^{-2}.

The spectral distributions of the all-sky fluxes of the GAT atmosphere are presented in Fig. 26. The all-sky spectral GE shown in Fig. 27. The numerical values of the integrated fluxes show that the GAT atmosphere is practically a radiative equilibrium structure.

Evidently, the all-sky greenhouse effect locked to the reflected solar radiation: $G^A = 103.0418$ Wm^{-2}, and $F_R = 103.032$ Wm^{-2}. The clear sky g locked tightly to $\tau_A^T : (S_U - OLR)/S_U = 0.33684$, $g(\tau_A^T) = 0.3382$. In Fig. 26 superscripts are references to the NASA planetary fact sheets, NASA GSFC NSSDC (2012). For reference, in Table 2 the detailed numerical results of the equilibrium flux density components are shown. The Kirchhoff rule seems to be perfectly satisfied. The $A_A^C = OLR$ and $E_D^C = OLR^C$ equalities put the full control of the planetary radiative equilibrium into the hand of the global average cloud cover.

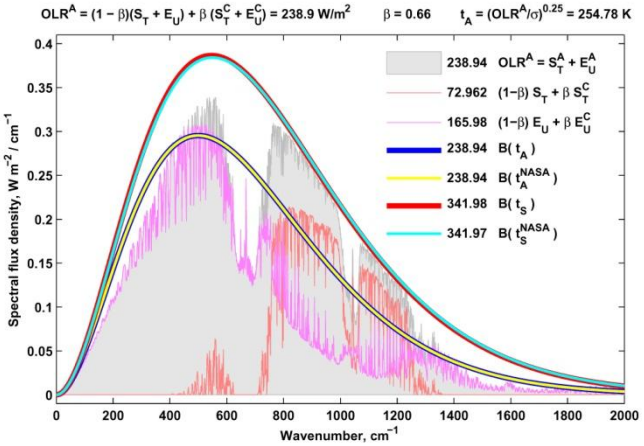

FIG. 26 FLUX DENSITY SPECTRA OF THE ALL-SKY GAT ATMOSPHERE. THE EQUIVALENT BLACKBODY SPECTRA $B(t_A)$, AND $B(t_S)$ ARE EQUAL TO THE EQUIVALENT BLACKBODY SPECTRA OF $B(t_A^{NASA})$, AND $B(t_S^{NASA})$.

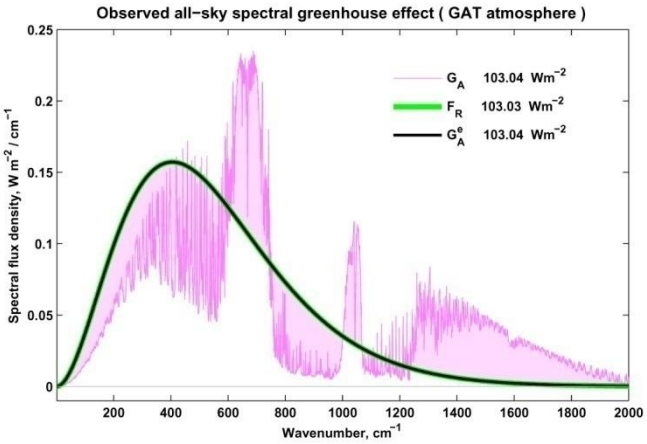

FIG. 27 SPECTRAL ALL-SKY GREENHOUSE EFFECT G_A. F_R AND THE EFFECTIVE G_A^e AGREE REASONABLY WELL.

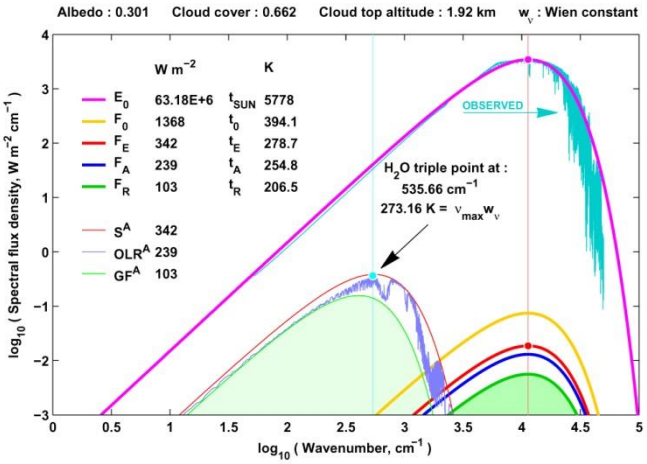

FIG. 28 SOLAR AND TERRESTRIAL EQUILIBRIUM BLACKBODY SPECTRA. THE LIGHT BLUE CURVE IS THE SOLAR SPECTRUM, THE DARK BLUE IS THE OBSERVED LW SPECTRAL OLR^A FROM THE GAT ATMOSPHERE. THE CYAN DOT MARKS THE MAXIMUM OF THE 273.15 K BLACKBODY SPECTRUM.

TABLE 2. GAT HIGH ACCURACY BOUNDARY FLUXES IN WM^{-2} . REGION BOUNDARIES ARE IN KM. IN CLOUDY ATMOSPHERE THE $A_A^C = OLR$ (RED) AND $E_D^C = OLR^C$ (GREEN) EQUALITIES ARE ONLY SATISFIED AT A SINGLE $h^C = 1.916$ KM ALTITUDE.

REGION	UPWARD			DOWNWARD
	S_U	A_A	OLR	E_D
0-70	379.69	321.12	251.79	309.93
1.92-70	333.82	251.12	240.14	240.15

Considering the temporal and areal variability in the local water vapor content of an air column, one has to admit that the Earth's atmosphere possesses enormous stability against fluctuations in its global average flux optical thickness. In our understanding, the source of this stability is related to two natural causes. One is the favourable orbital parameters of the Earth, and the other is the permanent presence of the three phases of the H_2O in the boundary layer. According to the Maxwell rule, the system as a whole has zero thermodynamic degree of freedom, the phase temperature of the system must be the triple point of the H_2O (273.16 K). In Fig. 28 we demonstrate, that the maximum of the all-sky thermal emission spectrum of the planet is, in fact, a spectral distribution of maximum radiation entropy.

Conclusions

In this research the IR radiative processes in the climate system are studied quantitatively. Observed empirical facts point to the existence of a climate invariant constant global average clear sky flux optical thickness of $\tau_A = 1.87$. Theoretical support has also been established with four fundamental radiative transfer relationships and a theoretical $\tau_A^T = 1.8676$ flux optical thickness. The clear sky $OLR = 251.79$ Wm^{-2} and $S_U = 379.69$ Wm^{-2} fluxes are fully consistent with the $OLR = S_U f(\tau_A^T)$, and the $OLR = S_U (0.6 + 0.4 T_A^T)$ theoretical requirements. It is also shown that the global average atmosphere with its effective cloud layer at $h^C = 1.9160$ km and a geometric cloud fraction of $\beta = f(\tau_A^T) = 0.6618$ is in radiative balance with the $F_E = 341.97$ Wm^{-2} TOA available solar radiation. It has been proven quantitatively that the conservation of radiant energy is established by the $\alpha_B = g^A = 0.3013$ and $\beta = f(\tau_A^T) = 0.6618$ equalities. In this respect the two equations linking the Bond albedo to the cloud cover and the all-sky normalized greenhouse factor have fundamental importance. As long as the Earth has unlimited water supply (in the oceans) with its three phases permanently present in the atmosphere and two phases on the ground surface, the stability of the planetary climate will be controlled by the $\beta = (G - \alpha_B F_E)/(G - G^C)$ and $\alpha_B = (G - \beta(G - G^C))/F_E$ equations. These two equations, together with the Clausius-Clapeyron equation, will regulate the transfer of the latent heat through the boundary layer in such a way that the net amount maintains the planetary radiative balance. In this regard the thermodynamic boundary layer may be defined as the combined surfaces where the different phases of the water are in direct physical contact with each other and with the surrounding material.

The apparent role of the Clausius-Clapeyron equation is to convert temperature differences to radiative fluxes (to and back), and by doing so to assure that no temperature-radiation feedback exists in the system. The only solution to the Earth's ground surface temperature is $t_G = (S_U/\sigma/\varepsilon_1)^{1/4} = 288.6 \pm 0.1$ K. The $t_P = (t_M + \varepsilon_1^{1/4} t_G)/2$ phase temperature is 273.17 ± 0.1 K, where $t_M = \sigma t_M^4 = \sigma^{-1/3} = 260.29$ K is a unique universal temperature. The empirically established climatological normalized GF of $g_m^A \approx 0.4$ is also reproduced well and proved by the $g_m^A = 1 - OLR^A/\sigma t_G^4 = 0.3992$ equation.

Of course the whole dynamically controlled system has no real instantaneous equilibrium state. However, the radial (or mass) oscillation of the system will be able to handle the energy conservation and energy minimum principles as required by the time constants of the different latent heat reservoirs. In summary, the complex task of the relatively fast responding global mean cloud cover is to assure the conservation of radiant energy and momentum on a global scale, maximize the LW cooling to space (radiative equilibrium), while observing the thermodynamic constraints applicable to large heterogeneous systems (Maxwell rule).

The quantitative proof of the radiative equilibrium state of the Earth-atmosphere system is alone a remarkable achievement of planetary science. The proposition here is to consider the global average cloud cover as the only component of the climate system, which is able to respond to and regulate the planetary radiation budget in a relatively short time. The greenhouse effect of the Earth's atmosphere is a global scale equilibrium process which rests on the chaotic nature of the humidity field and the stability of

the total atmospheric mass. Consequently, none of any local or regional weather phenomenon is related directly to its magnitude and tendency.

Unfortunately the Nobel Laureate IPCC is not a scientific authority, and their claim of the consensus and the settled greenhouse science is meaningless. The quantitative results of this paper massively contradict the CO_2 greenhouse effect based AGW hypothesis of IPCC.

In our view the greenhouse phenomenon, as it was postulated by J. Fourier (1824), estimated by S. Arrhenius (1906), first quantified by S. Manabe and R. Wetherald (1967), explained by R. Lindzen (2007), and endorsed by the National Academy of Science and the Royal Society (2014), simply does not exist.

However, research must continue to find and establish the real causes and the true trends in global temperature change that may be present behind the natural fluctuations. The greenhouse science is not settled, the presented results warrant further efforts to investigate many detailes of the surface radiative equilibrium processes.

ACKNOWLEDGEMENTS

I am very grateful for the help and support obtained from K. Gregory, and C. Game. Without their computational assistance, this research project could not exist. I also wish to thank K. Vinnikov, A. Rörsch, D. Hagen, S. Welcenbach, C. Wiese, G. Fulks, D. Brooks, W. Guang, Y. Shaomin, L. Szarka, V. Wesztergom, Sz. Barcza, Z. Kollath, Z. Toth, S. Kenyeres and P. Nemeth, for their continuous attention and valuable advice. The help and scientific contributions from my two friends, N. VanAndel and J. Pompe, who both died while in the midst of this work should also be remembered. Credit also go to C. Dubay, E. Carbone and J. Ginsberg for their help with the technical editing of the manuscript. The work of the reviewers and the editors of the journal is highly appreciated.

REFERENCES

Arrak, Arno. "Arctic warming is not greenhouse warming" Energy and Environment 22, 8 (2011) 1069-1083

Arrak, Arno. " What Warming? Satellite view of global temperature change" Second edition, CreateSpace, 2010

Arrhenius, S. "On the Influence of Carbonic Acid in the Air upon the Temperature of the Ground. " Philosophical Magazine and Journal of Science 5,41 (1896) 237-276.

Chandrasekhar, S. " An Introduction to the Study of Stellar Structure " 51-53, Dover Publications, 2010

Chedin, A., and Scott, N., A. " The Improved Initialization Inversion Procedure (3I)" Laboratoire de meteorologie dynamique, CNRS, Note Interne No. 117, LMD, 1983

Clausius, R., J., E., 1870: On a mechanical theorem applicable to heat ; Philosophical Magazine, 4,40 (1870) 127

Costa, S., M., S., and Shine, K., P. "Outgoing Longwave Radiation due to Directly Transmitted Surface Emission" Journal of the Atmospheric Sciences 69 (2012) 1865-1870

Cox, J., P., and Giuli, R., T."Principles of Stellar Structures" 408, Gordon and Breach Science Publishers, 1968

De Bruin, H., A., R." Comments on 'Greenhouse effect in semi-transparent planetary atmospheres' by Ferenc M. Miskolczi." Időjárás 114, 4 (2010) 319-324

ERBE Monthly Scanner Data Product. NASA Langley Research Center, Langley DAAC User and Data Services 2004, userserv@eosdis.larc.nasa.gov

Gerlich, G., and Tscheuschner, R., D."Falsification Of The Atmospheric CO_2 Greenhouse Effects Within The Frame Of Physics." International Journal of Modern Physics, B, 23, 3 (2009) 275-364 , doi:10.1142/S021797920904984X

Fourier, J. "Remarques générales sur les températures du globe terrestre et des espaces planétaires." Annales de Chimie et de Physique 27 (1824) 136-167

Hansen, J., et al. "Climate impact of increasing atmospheric carbon dioxide." Science 213 (1981) 957–966.

Hertzberg, M. "Earth's radiative equilibrium in the solar irradiance." Energy and Environment 20,1 (2009) 83-93

HITRAN2K, (2002) . http://cfa-www.Harvard.edu/HITRAN /hitrandata

Kiehl, J., T., and Trenberth, K.,E. "Earth's Annual Global Mean Energy Budget." BAM S 78(2), (1997) 197-208

Kimoto, K. "On the confusion of Planck feedback parameters." Energy and Environment 20,7 (2009) 1057-1066

Kratz, D., P., et al. "An Inter-Comparison of Far-Infrared Line-by-Line Radiative Transfer Models." JQSRT 90, (2005) 323-341

Lacis, A., Schmidt, G.A., Rind, D., Ruedy, R.A. "Atmospheric CO_2: Principal Control Knob Governing Earth's Temperature ." Science 330 (2010) 356-359

Lindzen, R., S. " Taking Greenhouse Warming Seriously." Energy & Environment 18 (2007) 937–950

Manabe, S., and Wetherald, R. "Thermal Equilibrium of the Atmosphere with a Given Distribution of Relative Humidity ." Journal of the Atmospheric Sciences 24,3 (1967) 242-259

Mihalas, D., and Weibel-Mihalas, B. "Foundations of Radiation Hydrodynamics.", 361, Dover Publications, Inc. Mineola, NY, 1999

Miskolczi, F., M. " High Resolution Atmospheric Radiative Transfer Code (HARTCODE) ." Technical Report. IMGA-CNR, Modena, Italy, 1989

Miskolczi, F. M. and Mlynczak, M. G." The Greenhouse Effect and the Spectral Decomposition of the Clear-Sky Terrestrial Radiation." Időjárás 108,4 (2004) 209-251

Miskolczi, F.M. "Greenhouse effect in Semi-transparent Planetary Atmospheres." Időjárás, 111,1 (2007) 1-40.

Miskolczi, F.M. "The stable stationary value of the earth's global average atmospheric Planck-weighted greenhouse-gas optical thickness" Energy & Environment 21,4 (2010) 243-262

Miskolczi, F.M. "The stable stationary value of the earth's global average atmospheric infrared optical thickness" EGU 2011 Vienna, http://presentations.copernicus.org/EGU2011-13622_presentation.pdf

Miskolczi, F. M. "Energetikai Kényszerek az Üvegházhatás Kialakulásában." Hungarian Academy of Sciences (2014) http://csfk.mta.hu/csfkwp/wp-content/uploads/2014/06/miskolczi_greenhouse_2.pdf

NASA, GSFC, NSSDC. NASA Official: Ed Grayzeck, edwin.j.grayzeck@nasa.gov, LastUpdated: 02 March 2012 http://nssdc.gsfc.nasa.gov/planetary/factsheet

NOAA, NASA, USAF. " U.S. Standard Atmosphere, 1976." U.S. Government Printing Office, Washington D. C. 20402, NOAA-S/T 76-1562, 1976

NOAA NCEP/NCAR Reanalysis data time series 2008, http://www.cdc.noaa.gov

Pierrehumbert, R.,T. "Principles of Planetary Climate." 189, Cambridge University Press, 2010

Pierrehumbert, R.T. "Infrared radiation and planetary temperature ." Physics Today Jan. (2011) 33-38

Ramanathan, V. "The role of ocean-atmosphere interactions in the CO_2 climate problem." Journal of the Atmospheric Sciences 38 (1981) 918–930.

Ramanathan, V., and Inamdar, A.,K. "The radiative forcing due to clouds and water vapor." In Frontiers of Climate Modeling Eds. J.T. Kiehl and V. Ramanathan; Cambridge University Press, 2006.

Raval, A., and Ramanathan, V. "Observational determination of the greenhouse effect." NATURE 342 (1989) 758-761

Real Climate (2008). http://www.realclimate.org/index.php/archives/2008/04/egu-2008/comment-page-2/

Rodriguez, R., et al. "Model, software, and data-base for computation of line-mixing effects in infrared Q branches of atmospheric CO_2. I. Symmetric isotopomers." JQSRT 61 (1999) 153-184

Science of Doom 2014: http://scienceofdoom.com/2014/06/26/the-greenhouse-effect-explained-in-simple-terms/

Spencer, R., W. "Comments on Miskolczi's (2010) Controversial Greenhouse Theory." 2010, http://www. drroyspencer.com/2010/08/

Stephens G., L., et al. "An update on Earth's energy balance in light of the latest global observations." Nature. Geoscience. 5 (2012) 691–696 doi:10.1038/ngeo1580

TIGR, Thermodynamic Initial Guess Retrieval 2000, http://ara.lmd.polytechnique.fr/htdocs-public/products/TIGR/TIGR.html

Toth, V. "The virial theorem and planetary atmospheres. Időjárás 114,3 (2010) 229-234

Trenberth, K., E. "Atmospheric reanalyzes : A major resource for ocean product development and modeling." Community White Paper, 30 March 2009, Revised 6 August 209, Lead author Kevin E. Trenberth, NCAR, P. O. Box 3000, Boulder CO, 80307

Trenberth, K.,E., Fasullo, J.,T., Kiehl, J. "Earth's Global Mean Energy Budget." BAMS March (2009) 311-323

Ollila, A. "Earth's Energy Balance for Clear, Cloudy and All-Sky Conditions." Development in Earth Science, Vol.1, Issue 1, September, 2013, www.seipub.org/des

Royal Society and the US National Academy of Sciences, An overview. "Climate Change : Evidence & Causes." 2014, http://dels.nas.edu/resources/static-assets/exec-office-other/climate-change-full.pdf

Van Andel, N. "Note on the Miskolczi theory." Energy and Environment 21, 4 (2010) 277-292.

Wild, M. et al. "The global energy balance from a surface perspective." Clim. Dyn. 40 (2013) 3107–3134, doi: 10.1007/s00382-012-1569-8

Ferenc Miskolczi Born in Budapest, Hungary in 1947. At the Eötvös Loránd University, Budapest, he earned an MS degree in nuclear physics (1971), and a PhD degree in astrophysics (1975). At the Hungarian Academy of Sciences he earned another PhD in Earth Sciences (1981). He also holds a diploma in high-level computer programming.

He specialized in the experimental and theoretical aspects of infrared atmospheric radiative transfer. During the 80s, and 90s, he taught and did research at several universities. Before his international career, he was the head of the Department of Atmospheric Radiation at the Institute of Atmospheric Physics, Budapest (Hungary). He was a research associate in the International Centre for Theoretical Physics, Trieste (Italy), a research scientist of the University of Maryland (USA), BSRN Staion Scientist in Ilorin (Nigeria), and a senior principal scientist at the Raytheon STX Corporation (USA).

He worked as Co-Principal Inveestigator on several NASA projects related to the problems of atmospheric remote sensing and planetary radiation budget. In 2003 he discovered and established the equations governing the infrared radiative transfer in semi-transparent atmospheres. In 2006 he resigned from NASA in protest due to unresolved publication issues related to his AGW related results. Recently his research interest has been the planetary greenhouse effect. His new idea of the greenhouse effect is getting more and more widely recognized. He is Foreign Associate Member of the Hungarian Academy of Sciences.